國立臺灣大學生物資源暨農學院森林環境暨資源學系
碩士論文
School of Forestry and Resource Conservation
College of Bioresources and Agriculture
National Taiwan University
Master’s Thesis

臺灣西南部鰲鼓海岸溼地造林及農地土壤鹽化與生態系碳吸存之權衡

Trade-offs between Soil Salinization and Ecosystem Carbon Sequestration in Afforested and Crop Lands of Aogu Coastal Wetland, Southwest Taiwan

沈樂恩
Yao-En Shen

指導教授：鄭智馨 博士
Advisor: Chih-Hsin Cheng, Ph.D.

中華民國 114 年 7 月
July, 2025

doi:10.6342/NTU202502856

國立臺灣大學碩士學位論文
口試委員會審定書
MASTER'S THESIS ACCEPTANCE CERTIFICATE
NATIONAL TAIWAN UNIVERSITY

臺灣西南部鰲鼓海岸濕地造林及農地土壤鹽化與生態系碳吸存之權衡

Trade-offs between Soil Salinization and Ecosystem Carbon Sequestration in Afforested and Crop Lands of Aogu Coastal Wetland, Southwest Taiwan

本論文係沈樂恩（R13625009）在國立臺灣大學森林環境暨資源學系完成之碩士學位論文，於民國 114 年 7 月 22 日承下列考試委員審查通過及口試及格，特此證明。

The undersigned, appointed by the School of Forestry and Resource Conservation on 22 July 2025 have examined a Master's Thesis entitled above presented by Yao-En Shen (R13625009) candidate and hereby certify that it is worthy of acceptance.

口試委員 Oral examination committee:

鄭智馨　　江博能　　陳尊賢

（指導教授 Advisor）

系（所、學位學程）主管 Director: 丁宗蘇

誌謝

以前看著學長姐論文中的謝誌，彷彿他們帶著我回到過去，一起回顧在實驗室的歷史，沒想到現在輪到我了，感覺有點奇妙。能夠完成一篇碩士論文，真的很不容易，一路上受到好多人的幫助與支持，我有說不盡的感謝。

首先謝謝鄭智馨老師，在我大二升大三的暑假，就給我機會進入研究室，並一起參與、學習研究工作。大三升大四時，幫助我申請大專生計畫，並在之後越來越繁重的研究工作中，詳細、嚴謹得指導我，無論是實驗的操作、文獻的查詢與閱讀，以及論文的寫作，我都獲益良多。謝謝鄭老師的耐心與包容，在我急躁、迷惘，甚至不知所措的時候，幫助我釐清下一步該怎麼走。也謝謝陳尊賢老師與江博能博士願意擔任我的口試委員，並給予我很多研究思考、論文寫作上的建議，幫助論文更加完善。

研究的生活很多時候相當枯燥、無聊，有時又忙到爆炸，若不是實驗室夥伴們的支持，我真的不知道還要多久才能走到碩論完成的這天。謝謝子穎在我進研究室時給我的支持、幫助，教導我許多儀器的操作，還有陪我閒聊，一起度過許多有趣的時光；謝謝笙翰在論文收尾階段給我的建議。謝謝從大學部就一起進研究室，到後來又一起變成研究生的昇祐，陪我採樣、幫助我操作實驗儀器，還有與我吃飯聊天，你是我心目中永遠的小巨人。謝謝之後一起在研究所打拼的勝榮、政珉，以及後來的雲睎，不管是一起採樣、做實驗、討論、吃飯、聊天，你們都成為我很大的幫助。

謝謝爸媽一路上的支持，每當我遇到挫折時，你們總會聽我吐苦水、鼓勵我，幫助我找到方法繼續堅持下去，你們是我最堅強的後盾。謝謝教會、團契裡的每個朋友，你們的陪伴總是給予我很大的動力，使能夠繼續在研究路上向前行。

謝謝上帝，是祢在這一路上陪著我，帶領我走過高山與低谷，在我軟弱時成為我的力量，在黑暗中成為我的亮光。當我迷惘時，祢總是指引我走在當行的路上，並成為我的力量與幫助。願我能一生緊緊跟隨祢，直到永遠。

感謝國立臺灣大學生物資源暨農學院共同儀器中心協助本研究 SEM-EDS 的操作與使用。

doi:10.6342/NTU202502856

摘要

隨著氣候變遷與全球暖化日益嚴重，它們對自然與人類生存的影響也日漸顯著。其中，海平面上升與海水入侵已經造成沿海環境劣化的危機，包含土壤鹽化、海岸侵蝕，以及糧食安全等，對沿海的生態與人類生命財產生存帶來威脅。本研究以鰲鼓濕地森林園區及其鄰近地區為研究對象，旨在探討海水入侵與地層下陷後，海岸森林及農地土壤鹽化的程度、兩者的差異，還有評估生態系碳儲存的能力。鰲鼓濕地森林園區為 60 年前海埔新生地，後因海水入侵鹽化而逐漸廢耕。本研究將此區域分為五個樣區，由沿海至內陸大致上分別為鰲鼓濕地西側(AG West)、鰲鼓濕地東側(AG East)、笨港港口宮(BG)、港墘(GC)，以及高鐵嘉義站(HSR)，並在每個樣區中選擇造林地與持續耕作之農地採集土壤。每個樣區土壤採集由淺至深分為 0-20 cm、20-40 cm、40-60 cm、60-80 cm、80-100 cm ，除了高鐵樣區由於土壤質地較黏，所以採樣深度僅至 20-40 cm)。將土壤依照分層深度進行基本性質與鹽分含量化學分析，包括飽和水抽出電導度(saturated water extract electrical conductivity, EC_e)、交換性鈉飽和度(exchangeable sodium percentage, ESP)，以及土壤有機碳(soil organic carbon)濃度，此外也使用樣區表層土壤種植玉米進行盆栽試驗。

研究結果顯示，鰲鼓濕地森林園區及鄰近地區之林地、農地土壤 pH 皆屬於鹼化範圍，與土壤母質和海水入侵有關。在海岸森林土壤方面，在水平方向上以最靠海岸的 AG West 及 AG East 的鹽化程度最嚴重，屬於強烈鹽化(EC_e 大於 16 dS m^{-1})其次是 BG 和 GC，屬於中度鹽化(EC_e：4.1-8.0 dS m^{-1})，鹽化程度最輕的樣區則是最內陸的 HSR，屬於無鹽化土壤；垂直方向上，則是在大部分樣區中呈現下層土壤鹽化較嚴重的現象，海岸林土壤 ECe 明顯超過多數植物之耐鹽極限，其土壤交換性鈉含量和 ESP 等指標也都普遍呈現較靠海較高，顯示此區域的海水入侵方向有由沿海向內陸、由下層往上層的趨勢。農地土壤方面，所有樣區的土壤都呈現無鹽化的狀態，顯示人為控管、洗鹽措施，以及土地利用型差異等，會導致土壤鹽化程度的不同，並且人為干預自然環境，在某種程度上能有效減緩土壤因海水入侵而鹽化的現象。玉米盆栽試驗也反映出類似的結果與相關趨勢，造林與農地土壤所種植的玉米地上部高度、生物量皆是越內陸越高，且相同樣區中，農地土壤的玉米地上部高度和生物量普遍較造林土壤的玉米高。代表鰲鼓濕地土壤鹽化的程度，對於該區常見作物生長會產生明顯的影響。土壤有機碳儲存方面，林地土壤的有機碳濃度雖然較農地土壤高，但其總體密度卻較農地土壤低，因此一來一往下，兩者整體地下部有機碳儲存並無明顯差異。不過，林地生態系除了土壤碳儲存外，再加上林木生物量以及枯落物層的碳儲存後，整體碳儲存會明顯高

doi:10.6342/NTU202502856

於農地生態系，約可多出 72.5-187.0 ton C ha^{-1}，顯示土地利用對於生態系碳吸存能力的影響巨大。

綜合以上，由本研究結果可得知，在海水入侵、土壤鹽化的情境下，沿海土地利用呈現兩難的情況。若以造林的方式利用鹽化土壤，可得到碳吸存與生物多樣性等生態系統功能的服務，但卻無法阻止土壤鹽化，而犧牲糧食生產的可能；但是另一方面，若持續以洗鹽與灌溉的方式維持土壤於無鹽化的狀態，可以確保可耕地的利用與糧食安全，卻會放棄森林可能提供的各樣生態系統功能。如此的兩難困境，是未來沿海土地管理者需要面對與抉擇的重要議題。

Abstract

As climate change and global warming intensify, their impacts on natural and human systems are becoming increasingly evident. Among these, sea-level rise and seawater intrusion pose serious threats to coastal environments, leading to ecosystem shifts, soil erosion, and soil salinization. This study investigated the forest and cropland soils of the Aogu Wetland Forest Park in southwestern Taiwan to assess their salinization status, differences between land-use types, and ecosystem carbon storage.

Five study sites were selected along a coastal–inland gradient: the west side of Aogu Wetland (AG West, nearest to the coast), the east side of Aogu Wetland (AG East), Bengang-Kangkao Temple (BG), Gangcian (GC), and the Taiwan High-Speed Rail Chiayi Station (HSR, farthest inland). At each site, soil samples were collected from both afforested land and croplands at depths of 0-20, 20-40, 40-60, 60-80, and 80-100 cm, except for the HSR site where clayey conditions limited sampling to 20-40 cm. Soil physical and chemical properties, including electrical conductivity (EC), exchangeable sodium percentage (ESP), and soil organic carbon (SOC) content, were analyzed. Additionally, a maize pot experiment was conducted in a greenhouse to evaluate the impacts of soil salinity on plant growth.

The results indicated that forest soils in AG West and AG East were strongly saline (EC_e greater than 16 dS m^{-1}), while BG and GC showed moderate salinity (EC_e：4.1-8.0 dS m^{-1}), with salinity generally increasing with depth, suggesting inland and upward seawater intrusion. Cropland soils, however, showed minimal to no salinization, indicating that irrigation and management practices can effectively mitigate soil salinity. The pot experiment supported these findings, as maize grown in saline coastal forest soils exhibited reduced height and biomass compared to maize grown in inland or cropland soils. Furthermore, although forest soils had higher organic carbon concentrations than cropland soils, their lower bulk density resulted in similar soil organic carbon

doi:10.6342/NTU202502856

storage overall. Yet, the total ecosystem carbon storage of forests in this study was significantly higher than that of cropland ecosystem due to contributions from tree biomass and litter layers. Compared to croplands, the forest ecosystem in this study stores 72.5 to 187.0 ton C ha^{-1}, highlighting the significant influence of land use on ecosystem carbon sequestration potential.

In conclusion, while coastal soils are vulnerable to salinization under seawater intrusion, active management can reduce this issue to an extent. These results suggest a trade-off in managing coastal saline soils: whether to prioritize afforestation for enhanced ecosystem services, such as carbon sequestration and biodiversity, at the cost of reduced agricultural productivity, or to favor agricultural land management to secure food production while compromising some ecosystem functions.

Keywords: climate change, coastal afforestation, sea water intrusion, soil salinization, ecosystem carbon storage

doi:10.6342/NTU202502856

目次 Table of Contents

doi:10.6342/NTU202502856

doi:10.6342/NTU202502856

doi:10.6342/NTU202502856

圖次 Figure Index

doi:10.6342/NTU202502856

表次 Table Index

doi:10.6342/NTU202502856

Chapter 1 Introduction

1.1 Global Warming, Climate Change, and Sea Level Rise

As climate change intensifies and global warming worsens, the frequency and severity of climate-related disasters, including extreme temperatures, droughts, floods, heavy rainfall, and sea level rise, are also increasing (IPCC, 2023). According to the Sixth Assessment Report (AR6) by the Intergovernmental Panel on Climate Change (IPCC), recent climate changes have been primarily driven by excessive greenhouse gas emissions resulting from human activities. The report states that the global surface temperature during 2010–2020 was 1.1°C higher than in the pre-industrial period of 1850–1900 (IPCC, 2023). These changes are expected to have widespread negative impacts on both natural ecosystems and human societies, including food and water shortages, health risks, and biodiversity loss (IPCC, 2023).

Among the most closely linked consequences of climate change are rising temperatures, extreme precipitation, sea level rise, and soil salinization. Elevated greenhouse gas concentrations have accelerated global warming, leading to increased glacial melt. The resulting influx of meltwater into the oceans is causing sea levels to rise, contributing to land loss along many coastal regions. According to Cazenave and Cozannet (2013), approximately 70% of the world's beaches are already experiencing erosion and retreat. Other coastal landscapes, such as sea cliffs, wetlands, and river

doi:10.6342/NTU202502856

deltas, are similarly receding. Spencer et al. (2016) projected that 46–59% of the world's coastal wetlands may be lost by the end of this century due to sea level rise, posing substantial ecological and socio-economic threats.

Seawater flooding not only endangers the livelihoods of coastal populations but also accelerates soil erosion and environmental degradation, rendering agricultural lands increasingly vulnerable (Ohenhen et al., 2023). This often leads to farm abandonment and heightens the risk of food insecurity (Eswar et al., 2021; El Shinawi et al., 2022). Therefore, understanding how saltwater intrusion alters coastal soils and ecosystems has become critically important.

1.2 Soil Salinization

1.2.1 Types of Soil Salinization

Soil salinization is a condition where excess salts build up in the soil (Zhang et al., 2022). Causes of salt accumulation can be simply classified into two categories: primary salinization and secondary salination (Zhang et al., 2022). Primary salinization means that the salt is accumulated from parent rock material, while secondary salinization means that salt is accumulated from human activities in the form of inadequate irrigation management from low-quality (salty) water, overuse of fertilization, or human induced land use change that increase the potential of salt accumulation. (Eswar et al., 2021; Mirlas et al., 2022; Zhang et al., 2022).

doi:10.6342/NTU202502856

Recent sea level rise plays an important role to cause seawater-induced soil salinization in coastal areas (Eswar et al., 2021; Kirwan et al., 2025). Seawater-induced soil salinization can be classified as a secondary salinization since the accumulation of salt is mainly driven by the anthropogenic activities. One of the major mechanisms is the inundation of seawater to submerge land and accumulate salt in these coastal soils (van de Wal et al., 2024). The process commonly occurs in the lowland coastal soils, but can be triggered by storm surges (Nordio and Fagherazzi, 2024) or tsunami (Iqbal et al., 2018). Furthermore, the sea level rise can intrude and elevate the groundwater table as well. Thus, another pathway for seawater induced salinization is through the groundwater intrusion with seawater, where the salts enter to soil systems from belowground (Alfarrah and Walraevens, 2018). Studies in coastal regions such as the Turkish Black Sea coast and the Nile River Delta (Arslan and Demir, 2013; Ding et al., 2020) have shown that groundwater electrical conductivity (EC), a key indicator of salinity, has been exceeded the acceptable levels due to the seawater intrusion and severely cause soil salinization (Kirwan et al., 2025).

Land subsidence can be another driver of seawater induced salinization. According to a study on the sea level rise of US Atlantic coast (Ohenhen et al., 2023), the downward vertical movement of the land caused seawater to further intrude to inland . Similarly, land subsidence, in combination with sea-level rise and seawater intrusion,

doi:10.6342/NTU202502856

has been a key factor in both soil and groundwater salinization in Europe (van de Wal et al., 2024). Ohenhen et al. (2023) reported that the rate of land subsidence exceeding 3 mm per year poses significant threats to coastal environments. Flooding, seawater intrusion, soil erosion and salinization, and the loss of wetlands, coastal forests, and agricultural land have been proposed as the widespread and transregional risks associated with the land subsidence(van de Wal et al., 2024).

1.2.2 Types of Land Use

Evapotranspiration Differences Across Land-Use Types

Different types of land-use may influence soil salinity to varying degrees, largely due to the differences in water cycle, such as irrigation, water infiltration/leaching, transpiration and evaporation. Forest ecosystems typically exhibit higher evapotranspiration rates than croplands, leading to greater water consumption and potentially more salt accumulation in the soil. A study in Flanders, Belgium, for example, found that under equal rainfall conditions, forested areas had significantly higher evapotranspiration than agricultural lands, indicating a greater water demand in forests (Verstraeten et al., 2005). Similarly, a study in Victoria, Australia, by Adelana et al. (2015) found that forest soils retained more salt than agricultural soils, likely because higher evapotranspiration in forests concentrated salts in the soil. In addition, Nordio and Fagherazzi (2024) indicated that high evapotranspiration can transport salts upward

doi:10.6342/NTU202502856

into the root zone and topsoil and thus exacerbate salinization. Their simulations demonstrated that soil salinity in sandy loam could increase by 26% over 100 days under a potential evapotranspiration rate at 2.5 mm per day. On the contrast, the rainfall may decrease the salt accumulation. When the ratio of potential evapotranspiration to rainfall (ET_p/Rainfall) exceeds one, salinity tends to increase, while salinity may decrease when this ratio is less than one. However, high infiltration rate in forest ecosystems may play different role to reduce soil salinization.

Crop ecosystem may have different scenarios in affecting soil salinization. Irrigation with low-quality water has been proposed as the main driver to soil salinization in arid/semiarid regions (Mirlas et al., 2022). By contrast, irrigation with fresh water can enhance salt leaching and mitigate soil salinization. In Taiwan, Korea, China, salt leaching has been wildly applied in reclaimed fields and successfully leach out the salt (Yin et al., 2022) to improve crop production. For example, a leaching study on saline-sodic soil conducted by Wang et al. (1984) (王百祿等，1984) demonstrated that irrigation with fresh water reduced soil electrical conductivity (measured using a saturated paste extract) from 56.25 to 4 dS m^{-1}.

1.3 Examples of Seawater Intrusion into Groundwater Systems and Soil

In Taiwan, the soil salinization is most found in the coastal areas and induced by seawater. Thus, this section will focuse on examples of salinization caused by seawater

doi:10.6342/NTU202502856

intrusion. Two previously discussed case studies, one from Turkey (Arslan and Demir, 2013) and another from Egypt (Ding et al., 2020), illustrate how seawater intrusion gradually degrades groundwater and soil quality in coastal regions.

Arslan and Demir (2013) investigated the Black Sea coast of Turkey, where excessive groundwater extraction was identified as the primary cause of seawater intrusion, extending up to 4 km inland. Groundwater electrical conductivity (EC) exceeded irrigation standards, and seawater–groundwater mixing ratios reached 15.07% near the coast. Soil salinity also increased with depth, with EC values ranging from 1.06 to 7.02 dS m^{-1}. In addition, the study found signs of soil alkalization: soil pH ranged from 7.41 to 9.42, and exchangeable sodium percentage (ESP) ranged from 10.97 to 15.83%. Both values increased with proximity to the coast and soil depth, suggesting intensified chemical degradation. According to the study's criteria (ESP > 6%; pH > 7-8), some soils had reached extreme alkalinity, potentially exceeding the tolerance of most crops.

Ding et al. (2020) reported similar conditions in Egypt's Nile Delta, where low elevation, arid climate, and agricultural dependence on groundwater make the region highly vulnerable to seawater intrusion. The study projected that a 1-meter sea-level rise could submerge 32% of land and deplete one-third of groundwater resources. At 5 km inland, the seawater mixing ratio reached 37.63%, and soil salinity was more severe in

doi:10.6342/NTU202502856

deeper layers. Soils within 25 km of the coast were moderately to strongly saline (EC: 4.0-16.0 dS m^{-1}), while inland soils were slightly saline (EC: 2.0-4.0 dS m^{-1}). Over two years, soil ECe increased by 0.34 dS m^{-1}, with corresponding rises in Na^+ and Cl^- concentrations, highlighting the growing severity of salinization caused by seawater intrusion.

1.4 Impacts of Coastal Ecosystem Service by Soil Salinization

When seawater intrudes into the soil, it alters the original chemical composition and material makeup of the soil, which in turn leads to changes in the composition of organisms inhabiting it. These changes can impact biodiversity and biogeochemical cycles within the ecosystem, ultimately affecting the ecosystem services it can provide (Herbert et al., 2015; Haywood et al., 2020; Mazhar et al., 2022).

Vegetation and aboveground carbon dynamic

Salinization primarily impacts plants by altering the osmotic properties of the soil solution, making it more difficult for plants to absorb water. This induces water stress, inhibits plant growth, and reduces biomass accumulation. High concentrations of specific ions in saline soils can also be toxic to plants, disrupting physiological processes and damaging cell development. For example, excessive sodium can inhibit the uptake of essential cations like potassium and calcium, which are critical for plant growth (Wong et al., 2010; Zhang et al., 2021). Additionally, salinization and

doi:10.6342/NTU202502856

alkalinization often degrade soil structure, reducing nutrient mobility and availability. This impairs root growth and nutrient uptake, further constraining plant development (Wong et al., 2010; Cox et al., 2018).

Furthermore, plant community composition is also shifting in response to sea level rise and seawater intrusion. Wendelberger and Richards (2017) conducted a study in the Everglades National Park in southeastern Florida to investigate these impacts. They found that rising sea levels result in habitat loss for coastal vegetation, while seawater intrusion causes soil salinization, allowing salt-tolerant halophytes to gradually invade and displace salt-sensitive glycophytes. These twin pressures have significantly threatened the survival and restoration of 21 rare coastal plant species within the park. This case underscores how sea level rise not only alters landscape structure but also puts biodiversity at risk by reshaping ecological niches and competitive dynamics in vulnerable coastal zones.

A study by Smart et al. (2020) on the coastal forests of North Carolina's Albemarle-Pamlico Peninsula found that sea level rise has caused long-term osmotic stress from seawater intrusion, leading to the gradual death of salt-intolerant tree species. As a result, the vegetation has shifted toward salt-tolerant shrubs and herbaceous species (Wendelberger and Richards, 2017; Smart et al., 2020). The remaining standing dead trees, known as "ghost forests", mark the transformation of

doi:10.6342/NTU202502856

these ecosystems into salt marsh-like environments. This transition reduces vegetation structural complexity due to changes in plant composition (Chmura et al., 2003), and widespread tree mortality leads to a significant loss in aboveground biomass (Setia et al., 2013). Smart et al. (2020) estimated that forest-to-marsh conversion on the peninsula resulted in an aboveground biomass loss of 16.2 Mg ha^{-1} and a carbon storage loss of 0.13 Tg C.

Soil Organic Carbon Dynamic

Plants are the primary source of organic carbon input to soil, so reductions in plant biomass directly decrease soil carbon storage and disrupt carbon cycling. Elevated soil salinity lowers plant productivity, leading to diminished organic carbon inputs and a gradual decline in soil organic matter, which increases vulnerability to erosion and degradation (Mazhar et al., 2022; Wong et al., 2010).

Soil salinization also disrupts microbial communities and the decomposition and mineralization processes that govern soil organic carbon (SOC) dynamics. While reduced plant inputs decrease SOC directly, microbial responses to salinity are more variable. High salinity can suppress microbial activity, respiration, and enzyme function due to osmotic stress and ion toxicity (Wong et al., 2010; Ardón et al., 2018), slowing organic matter breakdown and potentially increasing SOC. Conversely, seawater intrusion may promote anaerobic respiration, enhancing decomposition and

doi:10.6342/NTU202502856

mineralization and leading to SOC loss (Marton et al., 2012; Mazhar et al., 2022). Over time, microbial communities may adapt to saline environments, restoring or even accelerating SOC turnover (Zahran, 1997; Li et al., 2021).

In addition, salinity alters soil physical structure. High salt levels can cause clay flocculation and aggregate formation, particularly in the presence of Ca^{2+} and Mg^{2+}, helping protect SOC from microbial degradation (Yao et al., 2022). However, excessive exchangeable Na^{+} disperses soil particles, breaks down aggregates, seals soil surfaces, and reduces water infiltration (Cox et al., 2018). These changes increase erosion risk, expose SOC to decomposition, and hinder plant regeneration, further limiting carbon input (Wong et al., 2010; Dong et al., 2022). Root death under salinity stress also compromises soil structure and erosion resistance (Bronick and Lal, 2005). Because organic matter is lighter, it is easily eroded from topsoil, leaving behind subsoil with lower fertility and higher mineralization (Ruehlmann and Körschens, 2009; Wang et al., 2022). This feedback loop accelerates SOC loss and soil degradation.

Food security

As the global population continues to grow, the demand for food is also increasing. However, the amount of arable land on Earth is limited. Under such circumstances, utilizing coastal areas, reclaimed tidal lands, or even land created through coastal reclamation becomes a feasible approach to expand agricultural land and increase food

doi:10.6342/NTU202502856

production. At the same time, agricultural ecosystems may also serve as a potential source of carbon storage, helping to reduce excess greenhouse gases in the atmosphere (Freibauer et al., 2004). However, the soils in these areas are often influenced by their surrounding environments and tend to contain high levels of salts or suffer from seawater intrusion. Excessive salinity significantly affects various soil properties, including moisture content, organic matter, and carbon-to-nitrogen ratio, as well as alters or damages microbial community structures, enzyme activity, and suppresses soil respiration (Kumar et al., 2022). As a result, excessive salt accumulation in soil can hinder crop growth, ultimately defeating the original purpose of cultivating coastal and reclaimed lands.

According to a review by Lim et al. (2020) on carbon sequestration in reclaimed tidal croplands in South Korea, high salinity in these lands imposes stress on plant survival, reducing organic matter inputs from vegetation and subsequently lowering soil organic carbon levels. This aligns with findings from coastal forests and wetland ecosystems discussed earlier (Wong et al., 2010; Smart et al., 2020). In salinized cropland soils, changes in microbial biochemical activity and physical structure affect carbon storage in ways similar to unmanaged soils. High salt and sodium concentrations suppress microbial activity, biomass, and enzyme function (Wong et al., 2010; Lim et al., 2020), potentially slowing down organic matter decomposition and indirectly

doi:10.6342/NTU202502856

promoting carbon accumulation (Setia et al., 2013). However, excessive sodium can also alter soil physical properties, leading to surface crusting and erosion that remove the carbon-rich topsoil. Additionally, it can damage soil aggregates, exposing previously protected organic matter to microbial decomposition—echoing the findings of Wong et al. (2010) and Cox et al. (2018).

Beyond South Korea in Northeast Asia, similar challenges are also found in Southeast Asia. Surveys conducted by Renaud et al. (2015) in Vietnam's Mekong Delta and Khanom (2016) in Bangladesh reveal that many farmers perceive agricultural productivity to have been negatively affected by seawater intrusion and soil salinization due to climate change, with expectations of worsening conditions in the future. Agricultural output has noticeably declined, and soil EC values have exceeded the tolerance limits of common crops. Rising salinity is also causing the loss of native food crops and biodiversity in coastal regions. Moreover, to maintain crop yields in increasingly degraded soils, excessive fertilizer application may exacerbate salt accumulation. Intensifying salinization also reduces soil cohesiveness, leading to severe erosion and loss of soil along riverbanks.

1.5 Mitigation and Adaptation of Soil Salinization

Several ways have been proposed to mitigate soil salinization. The specific methods typically include the following (Shahid et al., 2018; Mukhopadhyay et al.,

doi:10.6342/NTU202502856

2021; Kirwan et al., 2025):

(1) The quality of irrigation water plays a critical role in determining soil salinity levels. Using poor-quality water can introduce excessive salts into the soil, exacerbating salinization (Mirlas et al., 2022). Therefore, it is essential to avoid irrigation with saline or low-quality water to prevent additional salt accumulation. On the other hand, irrigating with salt-free or low-salinity water can help leach excess salts from saline soils (Burt and Isbell, 2005). Additionally, improving drainage efficiency is vital to ensure the removal of leached water and to prevent waterlogging (Eswar et al., 2021; Kirwan et al., 2025).

(2) Amendments of gypsum and liming materials (containing cation ions, $Ca^{2+}$and Mg^{2+}) to the soil (Cox et al., 2018) can be employed to replace excess exchangeable sodium ions (Na^{+}) in the soil. This will reduce the exchangeable sodium content and promote stable aggregate formation. These processes will improve both the physical and chemical properties of the soil, hence ameliorating soil salinization.

(3) Changes to salt-resistant crop types or use salt-tolerant crop varieties. and farming practices, such as planting salt-resistant crops (Rengasamy, 2010; Kirwan et al., 2025) or farming salt-tolerant crop varieties, is another approach. For example, Taiwan Climate-Smart Agriculture (CSA) focuses on sustainable, circular, and green means to enhance agricultural productivity and promote resilience and adaptability

doi:10.6342/NTU202502856

to climate change. Irrigation management, choosing crop varieties, and selecting cultivation sites are some examples of individual practices (楊純明，2013；吳以健，2020). These methods can reduce the impact of climate change on agriculture, and ensure food security and optimal utilization of land, and avoid excessive or mistaken use of natural resources, leading to additional environmental degradation.

(4) Ongoing land use with ecological restoration practices, such as agroforestry, involves growing salt-tolerant crops and salt-resistant trees. This allows natural ecological processes to operate, gradually removing excess salts in the soil while maintaining food production as well as providing carbon sequestration. Besides, halophytic plant culture can trap salts of the surplus soil within the plant (White and Kaplan, 2017), reduce salinization of the soil, improve the environment, provide wildlife habitats, conserve biodiversity, and even help in carbon sequestration.

1.6 Indicators of Soil Salinity and Sodicity

Several soil measurements are proposed to indicate the status of soil salinization, in which the electrical conductivity (EC) and ESP values are commonly used to classify soil salinity and sodicity, respectively.

(1) EC: the standard method of measuring EC is the saturated soil paste extraction (EC_e). According to the USDA classification, the following levels apply to EC_e values (Ullman, 2013; Gibson et al., 2021):

doi:10.6342/NTU202502856

0-2.0 dS m^{-1}: Non-saline

2.1-4.0 dS m^{-1}: Slightly saline

4.1-8.0 dS m^{-1}: Moderately saline

8.0-16.0 dS m^{-1}: Strongly saline

Greater than 16 dS m^{-1}: Extremely (very strongly) saline.

However, EC_e operates on a larger sample of soil and the operator must consider whether the water content of the sample has saturated, and there is vacuum filtration to the operation involved. More training and time is required. A very common employed procedure then, therefore, is the 1:5 ratio of soil-to-water diluted ($EC_{1:5}$) that measures conductivity. Even though this methodology is not conventional, it is quicker, less complicated, and allows for quick EC detection (Sonmez et al., 2008; Kargas et al., 2022). Because of that, the conversion factor (CF) between both methodologies is considerable, and usually, it is obtained by carrying out a linear regression to find the slope as a representative figure.

(2) ESP: Exchangeable Sodium Percentage (ESP) is determined by measuring the exchangeable sodium ions in the soil and calculating the percentage of sodium relative to the CEC (Havlin et al., 2005). Another indicator is exchangeable sodium ratio (ESR), which is the ratio of exchangeable sodium to the combination of exchangeable calcium and magnesium (Havlin et al., 2005, see Appendix).

doi:10.6342/NTU202502856

1.7 Objectives

This study aims to address the increasing challenges posed by seawater intrusion and soil salinization in coastal regions, with a particular focus on the influence of land-use practices. The primary objectives are:

(1) to assess the extent of soil salinization in the coastal areas of the Aogu Wetland under two distinct land-use types—afforested land and cropland;

(2) to compare key soil properties, including salinity, sodicity, and carbon storage, between these two land uses; and

(3) to evaluate the respective advantages and limitations of afforestation and agriculture under the projected impacts of climate change and global warming.

By addressing these objectives, the study aims to clarify the ecological trade-offs and potential benefits associated with managing saline soils through either natural forest restoration or agricultural practices.

doi:10.6342/NTU202502856

Chapter 2 Materials and Methods

2.1 Study Sites

The study area is located in the Aogu Wetland Forest Park (23°30'19"N, 120°07'03"E) and its surrounding regions, Chiayi County, southwestern Taiwan. The site is passed bythe Tropic of Cancer, and makes the area have a tropical/subtropic climate. The mean temperatures in January and July are 16.8 °C and 28.9 °C, respectively. The mean annual precipitation is 1,821.8 mm (中央氣象署，2021), which approximately 76.7% of the annual rainfall occurs between April and September (嘉義市政府，2001).

The coastal areas, like the Aogu area, used to be affected by soil salination. However, with the construction of new irrigation system that used fresh water from rivers or deep groundwater, along with the construction of ditches in the fields and dikes on the seashore, had successfully reduced the soil salinity and improve crop production. The area become one of a productive region for sugarcane cultivation. , alongside other land uses such as aquaculture, animal husbandry, and plain agriculture. However, over time, seawater intrusion led to significant environmental changes, including ponding, wetland formation, and increased soil salinization (Fig. 1). These shifts in land conditions ultimately led to widespread abandonment of cropland (林業及自然保育署，2018；農業試驗所，2023).

doi:10.6342/NTU202502856

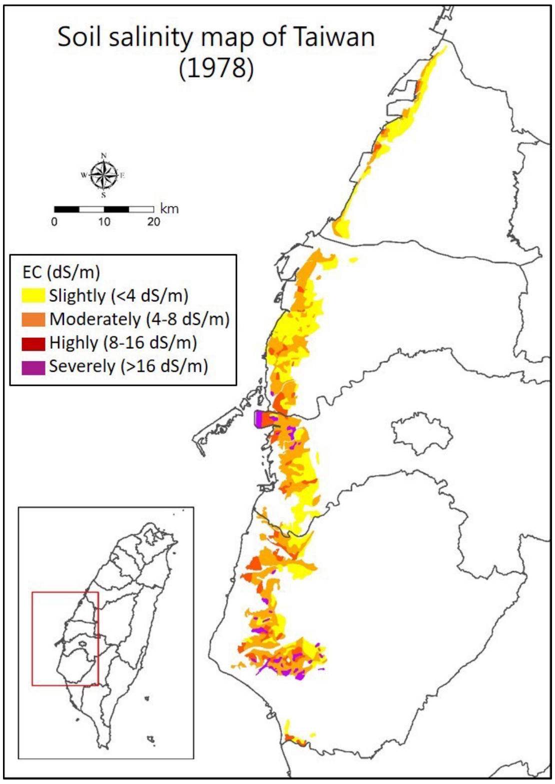

Fig. 1. Soil salinity in southwestern Taiwan. (農業試驗所，2023).
This graph illustrates soil salinity levels across southwestern Taiwan.
The Aogu Wetland is classified under the “Severely” category,
with electrical conductivity values exceeding 16 dS m^{-1} (shown in purple).

To restore the degraded landscape, an afforestation program was initiated in 2004 by the Taiwan Sugar Corporation and subsided by the Taiwanese government for potentially improving the ecosystem and creating the recreation park for civilians (Cheng et al., 2016). The project involved the conversion from sugar cane fields (*Saccharum* L.) into coastal forests. The afforested species in the Augo area were *Melaleuca cajuputi* (Maton & Sm. ex R.Powell), *Corymbia citriodora* ((Hook.) K.D.Hill & L.A.S.Johnson), *Casuarina equisetifolia* (L.) and *Palaquium formosanum*

doi:10.6342/NTU202502856

(Hayta). These species were well known for the tolerance of salt and wind, and were assumed to be well grown in sodic environments. The tree seedlings were initially planted at 1,500 seedlings per hectare with space at 3.6 m (row distance) x 1.8 m (seedling distance). The same species seedlings were planted in the same block. The whole areas looked like the mosaic pattern and intermitted with different tree species blocks. In additional to plantations, some areas were kept for annual cropping. Maize (*Zea mays* (L.), silage corn), green manure (*Crotalaria juncea* (L.), sun hemp; *Sesbania cannabina* (Retz.) Poir.), and paddy rice (*Oryza sativa* (L.)) were most common crop in the area (Table 1)Table

In the beginning of afforestation, the plantation was well maintained with irrigation, fertilization and weeding. However, those silvicultural managements, except for weeding, were not practiced after canopy close. With time, ocean inundation from broken dike, storm surge, land subsidence, and water logging from clogging ditch were found and gradually degraded the area. Some perimeter areas of Aogu Wetland Forest Park today were invaded with salty marshes or inundated with seawater. However, vigor plantation and crop fields still present.

doi:10.6342/NTU202502856

Table 1. Afforestation Characteristics of Aogu Wetland and Adjacent Areas

	AG West	AG East	BG	GC	HSR
Forests					
Plot number	5	5	3	3	3
Species	*C. equisetifolia* *C. citriodora* *M. cajuputi*	*C. equisetifolia* *C. citriodora* *M. cajuputi*	*C. equisetifolia* *C. citriodora* *M. cajuputi*	*C. equisetifolia* *C. citriodora* *M. cajuputi*	*S. macrophylla*
Density (no. ha^{-1})	1083.3 ± 370.4 A[a]	983.3 ± 123.0 A	983.3 ± 239.2 A	850.0 ± 93.5 A	925.0 ± 127.5 A
Mean DBH (cm)	17.8 ± 5.4 AB	17.2 ± 6.2 B	21.9 ± 9.1 AB	22.7 ± 6.4 A	21.4 ± 5.3 AB
Mean Height (m)	10.9 ± 2.3 BC	10.1 ± 2.9 C	11.7 ± 3.6 BC	16.8 ± 5.6 A	15.0 ± 1.6 AB
Basal Area (m^2 ha^{-1})	29.5 ± 10.9 A	25.8 ± 8.0 A	43.5 ± 18.2 A	37.0 ± 5.7 A	35.2 ± 5.1 A
Cropland					
Plot numbers	3	3	3	3	3
Crops	*Z. mays* *C. juncea* *S. cannabina*	*Z. mays* *C. juncea* *S. cannabina*	*Z. mays* *C. juncea* *S. cannabina*	*O. sativa* *C. juncea* *S. cannabina*	*Saccharum* spp.

[a] Post hoc comparisons among different sites are indicated by different uppercase letters.

2.2 Soil Sampling and Analyses

To compare how land use affecting the soil salinization, we selected five sites in the Aogu Wetland and the nearby forests and croplands. From the coastline to inland area wereFig.: the western side of Aogu Wetland (AG West), the eastern side of Aogu Wetland (AG East), Bengang-Kangkao Temple (BG), Gangcian (GC), and the Taiwan High Speed Rail Chiayi Station (HSR). We assume that soil salinity decreases with the increasing distance from coast to line. At each site, two land-use types, forest and

doi:10.6342/NTU202502856

cropland, were sampledentified for the comparison between two land use types (Fig. 3).

For each site, at least three replicates at both forest and cropland were established. At each replicate, three 20 x 20 m plots were used for aboveground and belowground analyses. .For the soil samples, we collected soil samples with 5 interval from 0 to 20 cm, 20 to 40 cm, 40 to 60 cm, 60 to 80, and 80 to 100 cm. At each soil layer, soils were pooled from three locations. At each site, samples were collected at 20 cm intervals from 0 to 100 cm depth, yielding five composite layers (0-20 cm, 20-40 cm, 40-60 cm, 60-80 cm, and 80-100 cm) formed by pooling three replicates per depth. At HSR sites, where high clay content impeded deeper sampling, only the 20-40 cm layer was collected. Soil samples were air-dried for 2-3 weeks, manually ground, and sieved through a 2 mm mesh. Samples were then analyzed for physical and chemical properties, including bulk density, pH, texture, electrical conductivity (EC), cation exchange capacity (CEC), exchangeable sodium percentage (ESP), and soil organic carbon (SOC).

doi:10.6342/NTU202502856

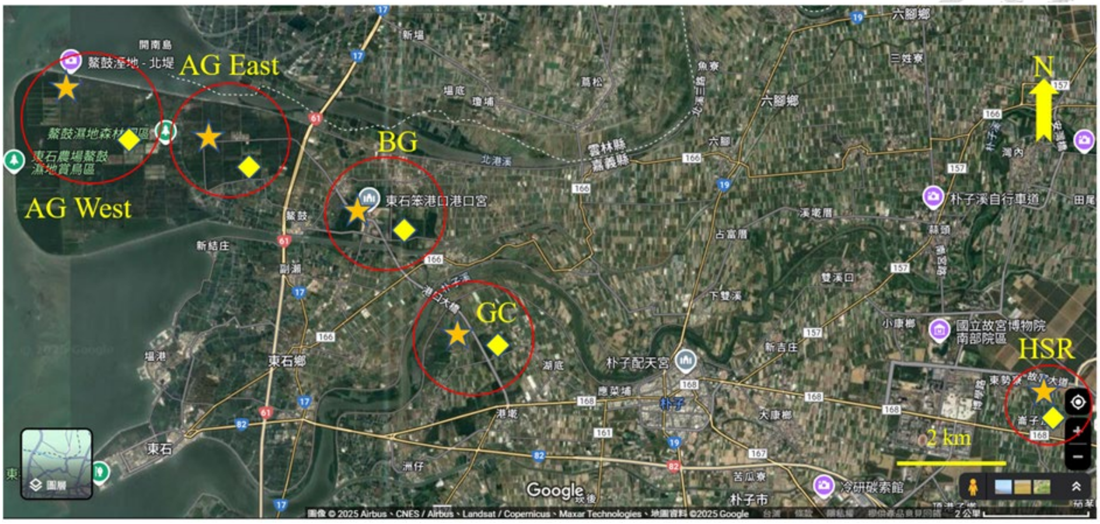

Fig. 2. Sampling sites. The five sampling areas, arranged from the coast to inland, are AG West, AG East, BG, GC, and HSR. Forest sites are marked with orange stars, while cropland sites are indicated by yellow diamonds. (Source: Google Maps)

Fig. 3. Coastal forest (left) and cropland (right) in Aogu Wetland.

2.3 Analyze Methods

2.3.1 Soil Properties

Bulk density was determined by oven-drying core samples (100 ml) collected at 0-20 cm and 20-40 cm depths at 105 °C for at least 24 hours and calculating the dry mass-to-volume ratio. Soil pH was measured in a 1:2.5 soil-to-water suspension (8 g soil, 20 ml distilled water) after shaking for 30 minutes and rest for another 30 minutes, using a

doi:10.6342/NTU202502856

glass electrode pH meter. Soil texture was analyzed via the hydrometer method (see formula 1a, 1b, and1c), with sand, silt, and clay percentages calculated based on standard hydrometer readings ($R_{40s'}$, $R_{7h'}$) corrected by blank values ($R_{L1'}$, $R_{L2'}$); the texture is then classified according to the soil texture triangle (USDA, n.d.; Groenendyk et al., 2015, Fig. 4). Electrical conductivity (EC) was measured both as saturated paste extract (EC_e) and in a 1:5 soil-to-water suspension ($EC_{1:5}$), with a conversion factor derived by linear regression (Khorsandi and Yazdi, 2011; Seo et al., 2022). Cation exchange capacity (CEC) was measured using an ammonia meter, and exchangeable cations (Na^+, Ca^{2+}, Mg^{2+}) were extracted with 1 M ammonium acetate and analyzed by flame atomic absorption spectrometry (GBC SensAA, Melbourne, Australia). Exchangeable sodium percentage (ESP) and exchangeable sodium ratio (ESR, Appendix, formula 3) was calculated using Na^+, Ca^{2+}, and Mg^{2+} concentrations according to standard formulas (formula 2). Some data from the HSR site were directly obtained from a previous study conducted at the same location (魏子穎，2024).

$$\text{sand } (\%) = 100 - (R_{40s'} - R_{L1'}) \times \frac{100}{\text{sample weight } (g)} \quad (1a)$$

$$\text{clay } (\%) = (R_{7h'} - R_{L2'}) \times \frac{100}{\text{sample weight } (g)} \quad (1b)$$

$$\text{silt } (\%) = 100 - (\text{sand } \% + \text{clay } \%) \quad (1c)$$

$R_{L1'}$: blank value of 40 seconds after calibration of temperature

$R_{L2'}$: the blank value of 7 hours after calibration of temperature

doi:10.6342/NTU202502856

$R_{40S'}$: measured value of 40 seconds after calibration of temperature

$R_{7h'}$: measured value of 7 hours after calibration of temperature

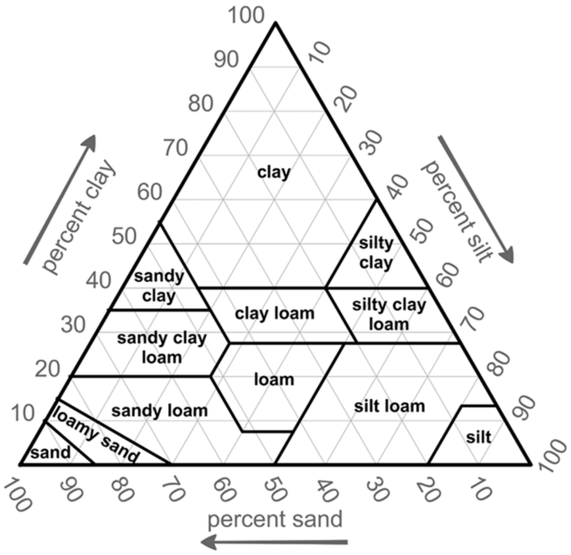

Fig. 4. Soil texture triangle (USDA, n.d.; Groenendyk et al., 2015).

$\mathrm{ESP} = \frac{Exchangeable\ Na^{+}}{CEC} \times 100\%$ (unit of concentration: cmol kg^{-1}) (2)

2.3.2 SEM-EDS Analysis

A JEOL JSM-6510LV Scanning Electron Microscope (SEM), equipped with an Oxford INCAx-Act Energy Dispersive Spectroscopy (EDS) system, was used to detect seawater-related ions in the soil (i.e., Cl, Na, K, Mg, and Ca). The analysis was conducted at the Joint Center for Instruments and Research, College of Bioresources and Agriculture, National Taiwan University. Soil samples were milled and sieved to retain particles ≤2 mm, then oven-dried at 60 °C for 7 days to remove moisture. After preparation, the samples were mounted on 1 cm diameter stubs using carbon tape and

doi:10.6342/NTU202502856

coated with gold. SEM-EDS analysis was performed with a working distance of 11 mm, a spot size of 70 μm, and an accelerating voltage of 25 kV.

2.3.3 Pot Experiment

Maize (*Zea mays* (L.); cultivar: Hua-Jen super sweet corn (超甜玉米-華珍)) was sown in both forest and cropland soils collected from six test sites, along with two control sites. The experiment was conducted from February 20 to April 3, 2024, lasting a total of 44 days. The six treatment groups included soils from the forest and cropland at three locations: AG West, AG East, and BG. The control soils, representing non-saline conditions, were collected from forested areas at the GC and HSR sites. Therefore, eight treatments were tested, each with eight replicates, that is, 64 pots in total.

The potting medium consisted of 2.5 kg of air-dried topsoil (0-20 cm), sieved through a 4 mm mesh and placed into 6-inch pots. Three maize seeds were sown in each pot and cultivated in a greenhouse at the National Taiwan University Experimental Farm. To maintain optimal soil moisture, pots were irrigated with fresh tap water once daily. This watering frequency aligns with findings from a recent study modeling maize irrigation in southwestern Taiwan, which estimated a seasonal irrigation requirement of 393.2 mm ha^{-1} during the dry season (許健輝等，2023). When seedlings reached the four-leaf stage, we thinned to one healthy seedling per pot. The maize was fertilized

doi:10.6342/NTU202502856

with #43 "HeyWon" Nitrophosphate Organic Compound Fertilizer (15-15-15 N–P_2O_5–K_2O) produced by Taiwan Fertilizer Co., Ltd. A basal application equivalent to 60 kg ha^{-1} was applied to each pot at the time of sowing. No additional fertilizer was applied during the remainder of the growing period.

During the experiment, seedling emergence was monitored and recorded. After 44 days, plant height was measured, and aboveground biomass was harvested. The harvested biomass was oven-dried at 65 °C for five days and weighed to determine dry mass. Plant height and dry biomass were used to evaluate the effects of different land-use types and soil salinity levels on maize growth.

The soil samples used to grow maize were collected at the time of harvesting. Soil samples were air-dried, manually ground, and sieved through a 2 mm mesh. Their EC was measured to determine the relationship of crop growth performance and soil salinity.

2.3.4 Ecosystem Carbon Storage

Ecosystem carbon storage was the summation of carbon pools in biomass, dead organic matter, and soils. We estimated biomass C stocks by measuring tree height and diameter at breast height (DBH) within 20 x 20 m plots, and calculated the biomass carbon using the i-Tree Eco (ver. 6.035) model (Kim et al., 2024). Dead organic matter was estimated by litter was collected from 0.5 x 0.5 m quadrats (Fig. 5), oven-dried, and

doi:10.6342/NTU202502856

converted using a carbon content coefficient of 0.47 (IPCC, 2006). Biomass and litter were assumed to be zero for croplands. To determine soil organic carbon (SOC) concentration, the carbonate content (inorganic carbon) in the soil samples was first removed using 1 M HCl, as the soils in the study area are derived from limestone parent material. The organic carbon concentration was then measured using an elemental analyzer (PerkinElmer 2400 II, Shelton, CT, USA). Soil organic carbon storage was calculated from bulk density and SOC concentration results (Table 2).

Fig. 5. 0.5 x 0.5 m quadrat for collecting litterfall.

2.3.5 Statistical Analysis

Statistical analyses were performed using R software (version 4.4.0). ANOVA was used to compare differences in soil properties between different sites within the same soil layer and between different layers within the same site. If there were large differences among data points or clear deviations from a normal distribution, the data

doi:10.6342/NTU202502856

were log-transformed (base 10) prior to statistical analysis.

If ANOVA indicated a significant difference ($p < 0.05$), a least significant difference (LSD) post hoc test was applied. In cases where no significant overall differences were detected (ANOVA, $p > 0.05$), LSD was still performed to examine the overlap in group means, with letter notation used to indicate non-significant pairwise differences for visualization purposes. Additionally, to compare different land-use types, values from each soil layer of forest and cropland soils were used, and an independent t-test was applied.

A Pearson correlation analysis was conducted to examine the relationships among different salinity indicators. Linear regression was applied to visualize and simplify the correlations between pairs of salinity indicators.

doi:10.6342/NTU202502856

Chapter 3 Results

3.1 Basic Properties of Soil from Aogu Wetland

3.1.1 Bulk Density

Bulk density ranges from 0.9-1.5 g cm^{-3} in forest soils and 1.0-1.5 g cm^{-3} in cropland soils. No clear lateral or vertical patterns were observed, except slightly lower density in the top 20 cm of forest soils. Cropland soils are generally denser, but the difference is not statistically significant. The HSR site shows notably higher values.

3.1.2 Soil pH

The pH values ranges from 6.1 to 9.4 in the study sites (Table 2). In general, the subsurface soil layers exhibit higher pH values than the surface layers, and the soils near the coast tend to have higher pH values than the inland soils. There is no significant difference in pH between forest and agricultural soils (Table 2).

3.1.3 Soil Texture

The soils near the coast generally exhibit a coarser texture, while those inland soils tend to be finer (Table 2). A trend of soil texture from sandy loam (AG West) to clay (HSR) can thus be found. Soil texture does not vary across the five soil layers, but the cropland soils s are generally coarser than their forest counterparts.

3.1.4 Cation Exchange Capacity (CEC)

CEC values range from 0.6 to 10.3 cmol kg^{-1} in forest soils, with HSR showing the

doi:10.6342/NTU202502856

highest value (>10 cmol kg^{-1}). In cropland soils, CEC ranges from 1.5 to 15.1 cmol kg^{-1}, with AG West showing the highest value. CEC does not vary notably across the five soil layers in either land use. When comparing land-use types within sites, significant differences occur only at AG West and GC, while no differences are found at AG East, BG, and HSR (Table 2).

3.1.5 Soil Organic Carbon (SOC)

SOC in forest soils ranged from 0.3% to 1.7% and ranged from 0.3% to 0.9% in cropland soils. Except for the HSR site which exhibited a notably higher SOC content, there is no clear pattern among other four sites. In both forest and cropland soils, the SOC in the 0-20 cm layer was generally higher than theoe in the deeper soils Although forest soils generally had higher SOC percentages than cropland soils, these differences are not statistically significant in most cases (Table 2).

doi:10.6342/NTU202502856

Table 2. Soil Basic Properties of Aogu Wetland

Soil Properties	Land Type	Depth (cm)	AG West	AG East	BG	GC	HSR
BD (g cm^{-3})	Forest	0-20	1.1 ± 0.1 Bb[ab]	1.0 ± 0.1 Bb	1.0 ± 0.1 Bb	0.9 ± 0.05 Ba	1.4 ± 0.02 Ab
		20-40	1.3 ± 0.04 Ba	1.3 ± 0.04 Ba	1.3 ± 0.03 Ba	1.1 ± 0.1 Ca	1.5 ± 0.1 Aa
	Cropland	0-20	1.2 ± 0.04 Cb	1.2 ± 0.02 Ca	1.2 ± 0.03 Cb	1.4 ± 0.1 Ba	1.6 ± 0.0 Aa
		20-40	1.4 ± 0.03 Ba	1.0 ± 0.02 Db	1.4 ± 0.02 Ba	1.2 ± 0.1 Ca	1.5 ± 0.0 Ab
Texture	Forest	0-20	Sandy loam	Silty loam	Silty loam	Sandy loam	Silty clay
		20-40	Sandy loam	Loam	Silty loam	Loam	Clay
		40-60	Sandy loam	Loam	Silty loam	Loam	-
		60-80	Sandy loam	Loam	Silty loam	Loam	-
		80-100	Silty loam	Silty loam	Silty clay loam	Loam	-
	Cropland	0-20	Sandy loam	Loamy sand	Sandy clay loam	Sandy loam	Sandy clay loam
		20-40	Sandy loam	Sandy loam	Loamy sand	Sandy loam	Loam
		40-60	Sandy loam	Sandy loam	Loamy sand	Sandy loam	-
		60-80	Sandy loam	Sandy loam	Loamy sand	Sandy loam	-
		80-100	Sandy loam	Sandy loam	Loamy sand	Loam	-
pH	Forest	0-20	6.9 ± 0.6 ABb	8.1 ± 0.1 Ab	7.7 ± 0.1 ABb	6.5 ± 0.5 Ba	7.1 ± 0.2 ABa
		20-40	8.7 ± 0.1 Aa	8.7 ± 0.3 Aa	8.2 ± 0.05 Aa	6.6 ± 0.4 Ba	7.2 ± 0.3 Ba
		40-60	8.8 ± 0.05 Aa	8.8 ± 0.1 Aa	8.3 ± 0.1 Ba	6.6 ± 0.3 Ca	-
		60-80	8.7 ± 0.1 Aa	8.4 ± 0.1 ABab	8.3 ± 0.1 Ba	7.3 ± 0.2 Ca	-
		80-100	8.7 ± 0.1 Aa	8.6 ± 0.1 Aab	8.2 ± 0.1 Ba	7.4 ± 0.1 Ca	-
	Cropland	0-20	8.9 ± 0.3 Aa	7.5 ± 0.3 Ba	7.1 ± 0.1 Bb	6.6 ± 0.6 Ba	7.1 ± 0.1 Ba
		20-40	9.3 ± 0.3 Aa	7.8 ± 0.6 Ba	7.8 ± 0.3 Bab	6.4 ± 0.5 Ca	6.4 ± 0.3 Cb
		40-60	9.4 ± 0.03 Aa	8.0 ± 0.6 ABa	8.1 ± 0.3 ABa	6.7 ± 0.5 Ba	-
		60-80	9.3 ± 0.2 Aa	8.1 ± 0.6 Aa	8.4 ± 0.3 Aa	6.5 ± 0.3 Ba	-
		80-100	9.3 ± 0.2 Aa	8.4 ± 0.2 Aa	8.3 ± 0.3 Aa	6.7 ± 0.3 Ba	-
CEC (cmol kg^{-1})	Forest	0-20	2.7 ± 0.7 Ba	2.3 ± 1.2 Ba	1.9 ± 0.7 Ba	3.5 ± 0.1 Ba	24.1 ± 0.6 Aa
		20-40	1.3 ± 0.5 Ba	3.9 ± 2.6 Ba	2.6 ± 1.0 Ba	3.2 ± 0.6 Ba	11.9 ± 2.3 Ab
		40-60	3.1 ± 0.8 Aa	2.1 ± 1.2 Aa	0.6 ± 0.2 Aa	3.7 ± 0.2 Aa	-
		60-80	2.0 ± 0.4 ABa	1.3 ± 0.7 Ba	1.2 ± 0.3 Ba	3.5 ± 0.4 Aa	-
		80-100	1.6 ± 0.6 Aa	6.0 ± 3.4 Aa	2.3 ± 1.0 Aa	4.4 ± 1.6 Aa	-
	Cropland	0-20	9.5 ± 3.3 Aa	3.5 ± 0.6 Ba	3.3 ± 1.5 Ba	2.5 ± 0.9 Ba	13.4 ± 1.3 Aa
		20-40	7.9 ± 4.0 Aa	4.5 ± 1.8 ABa	2.4 ± 0.7 ABa	2.2 ± 0.4 Ba	2.5 ± 0.3 ABb
		40-60	8.6 ± 2.5 Aa	1.7 ± 0.1 Ba	1.5 ± 0.5 Ba	2.5 ± 0.4 Ba	-
		60-80	15.1 ± 4.0 Aa	3.1 ± 1.0 Ba	1.9 ± 0.3 Ba	1.6 ± 0.2 Ba	-

doi:10.6342/NTU202502856

		80-100	10.2 ± 1.4 Aa	3.4 ± 0.5 Ba	1.8 ± 0.5 Ba	2.0 ± 0.4 Ba	-
SOC (%)	Forest	0-20	1.0 ± 0.2 ABa	0.9 ± 0.1 Ba	1.1 ± 0.2 ABa	1.0 ± 0.1 ABa	1.7 ± 0.5 Aa
		20-40	0.3 ± 0.02 Cb	0.4 ±0.01 Cb	0.6 ± 0.1 Ba	0.6 ± 0.04 Bb	1.0 ± 0.1 Aa
	Cropland	0-20	0.7 ± 0.1 ABa	0.6 ± 0.1 ABa	0.5 ± 0.1 Ba	0.7 ± 0.04 ABa	0.9 ± 0.05 Aa
		20-40	0.3 ± 0.1 Cb	0.4 ± 0.1 BCa	0.3 ± 0.01 BCa	0.5 ± 0.1 ABa	0.7 ± 0.02 Ab
TN (%)	Forest	0-20	0.1 ± 0.01 Ba	0.1 ± 0.01 ABa	0.2 ± 0.01 Aa	0.1 ± 0.01 ABa	0.1 ± 0.1 Ba
		20-40	0.1 ± 0.0 Cb	0.1 ± 0.0 BCb	0.1 ± 0.01 ABCb	0.1 ± 0.01 ABa	0.1 ± 0.1 Aa
	Cropland	0-20	0.1 ± 0.01 Aa	0.1 ± 0.01 ABa	0.1 ± 0.02 Ba	0.1 ± 0.01 ABa	0.1 ± 0.05 Ba
		20-40	0.1 ± 0.02 Aa	0.1 ± 0.01 Aa	0.1 ± 0.0 Aa	0.1 ± 0.01 Aa	0.1 ± 0.1 Aa
C/N ratio	Forest	0-20	9.1 ± 2.1 Aa	6.8 ± 0.6 Aa	7.0 ± 0.9 Aa	8.2 ± 0.9 Aa	11.0 ± 0.7 Aa
		20-40	3.4 ± 0.3 Cb	4.3 ± 0.1 Cb	5.5 ± 0.7 Ba	5.9 ± 0.2 Ba	8.7 ± 0.1 Ab
	Cropland	0-20	5.4 ± 0.1 Ba	5.3 ± 0.4 Ba	5.9 ± 0.4 Ba	6.0 ± 0.1 Ba	9.4 ± 0.3 Aa
		20-40	3.5 ± 0.4 Bb	4.4 ± 0.5 Ba	4.6 ± 0.4 Ba	5.3 ± 1.0 ABa	7.7 ± 1.3 Aa
Forest vs Cropland							
BD (g cm^{-3})	-	0-20	NS[c]	*	*	*	*
		20-40	*	*	*	p = NS	p = NA
pH	-	0-20	*	NS	*	NS	NS
		20-40	NS	NS	NS	NS	NS
		40-60	*	NS	NS	NS	-
		60-80	NS	NS	NS	NS	-
		80-100	NS	NS	NS	NS	-
CEC (cmol kg^{-1})	-	0-20	NS	NS	NS	NS	*
		20-40	NS	NS	NS	NS	*
		40-60	NS	NS	NS	NS	-
		60-80	NS	NS	NS	*	-
		80-100	NS	NS	NS	NS	-
SOC (%)	-	0-20	NS	NS	NS	NS	NS
		20-40	NS	NS	NS	NS	NS
TN (%)	-	0-20	NS	NS	*	NS	NS
		20-40	NS	NS	NS	NS	NS
C/N ratio	-	0-20	NS	NS	NS	NS	NS
	-	20-40	NS	NS	NS	NS	NS

[a] Different uppercase letters indicate significant differences among sites within the same soil layer (post hoc comparison).

doi:10.6342/NTU202502856

[b] Different lowercase letters indicate significant differences among soil layers within the same site (post hoc comparison).

[c] Independent t-tests were conducted to compare forest and cropland soils; results with $p < 0.05$ are labeled as *, while those with $p > 0.05$ are labeled as NS (not significant).

3.2 Salinity Properties of Soil from Aogu Wetland

3.2.1 Electrical Conductivities (EC) and Conversion Factor (CF)

The EC_e of forest soils ranges from 0.3 to 25.6 dS m^{-1}, while $EC_{1:5}$ ranges from 0.03 to 2.5 dS m^{-1} (Table 3). Both measurements exhibit a clear lateral trend, with EC values decreasing from coastal to inland sites within each soil layer. The Aogu Wetland sites (AG West and AG East) show the highest EC values, BG and GC sites are intermediate, and the HSR site has the lowest EC (Fig. 6 and Fig. 7). A vertical pattern is also observed within each site, in which the EC increases with depth, with the highest values found in the lower layers. This vertical gradient is more pronounced at coastal sites (AG West and AG East), whereas the more inland sites show less distinct variation across layers (Fig. 6). In cropland soils, EC_e ranges from 0.2 to 1.9 dS m^{-1}, and $EC_{1:5}$ from 0.03 to 0.2 dS m^{-1}. Unlike forest soils, cropland soils exhibit no consistent lateral or vertical trends in EC. The only exception is the GC site, where cropland soils have slightly elevated EC levels (Fig. 6 and Fig. 7).

doi:10.6342/NTU202502856

Significant differences in EC_e were observed between forest and cropland soils at the AG West and AG East sites (Table 3). At the BG site, although the difference in EC_e between forest and cropland soils was not statistically significant, the p-value approached the 0.05 threshold level. However, $EC_{1:5}$ at the BG site showed significant differences between forest and cropland soils in the lower three layers. No significant differences in EC were found between land-use types at the GC and HSR sites.

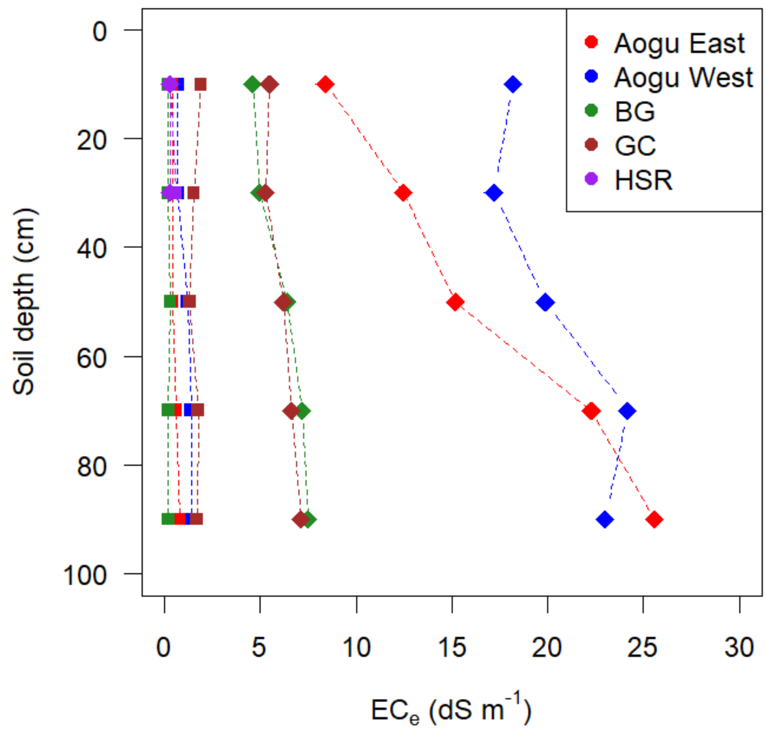

Fig. 6. Soil EC_e profiles by depth across study sites. Different colors represent different sites. EC_e values for forest soils are indicated by diamonds, while those for cropland soils are shown as squares. A vertical trend is observed in forest soils, with EC_e increasing from the surface to deeper layers. In contrast, cropland soils exhibit consistently low EC_e across all depths, showing no clear vertical pattern.

doi:10.6342/NTU202502856

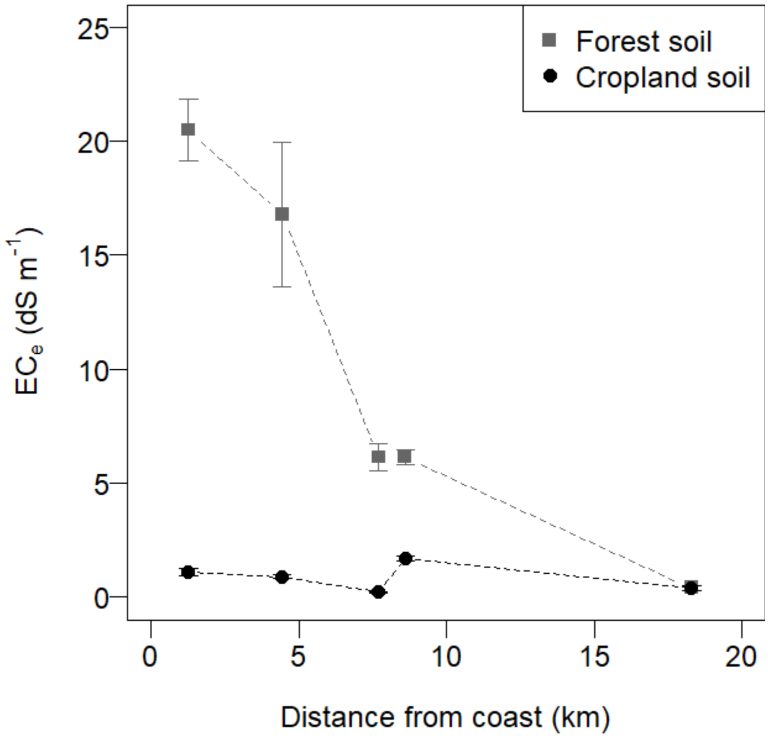

Fig. 7. Relationship between soil EC_e and distance from the coast to inland. Each point represents the mean EC_e across all soil layers at a given site. Forest soils are shown as gray squares, and cropland soils as black dots. Forest soil EC_e exhibits a clear decreasing trend with increasing distance from the coast to inland. In contrast, cropland soils maintain consistently low EC_e values with no apparent spatial pattern.

The conversion factor from $EC_{1:5}$ to EC_e in this study is 10.51 (Fig. 8), which is slightly higher than those reported in previous studies on sandy loam soils—7.98 by Sonmez et al. (2008), 9.55 by Gharaibeh et al. (2021), and 8.22 by Kargas et al. (2022).

doi:10.6342/NTU202502856

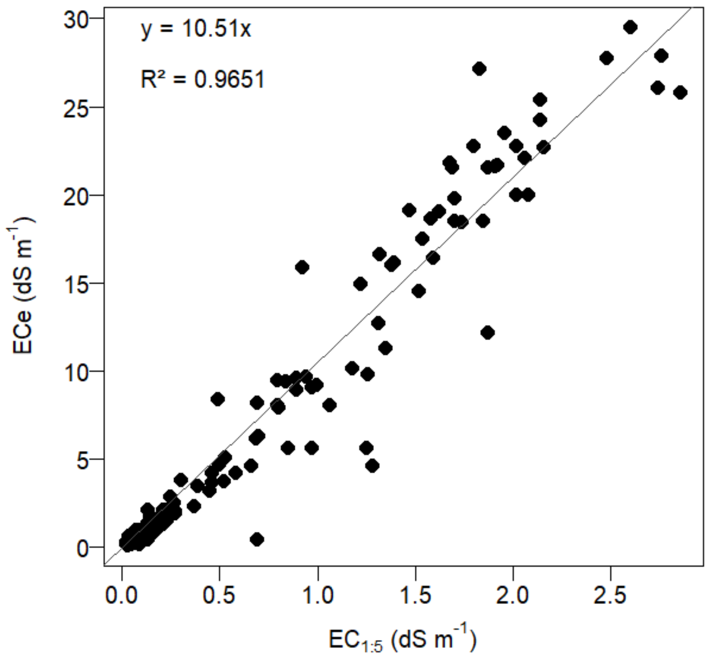

Fig. 8. The conversion factor (CF) between soil $EC_{1:5}$ and EC_e. The CF for Aogu Wetland is 10.51.

3.2.2 Exchangeable Cations

(1) Exchangeable Sodium:

Exchangeable Na^+ in forest soils ranged from 0.1 to 11.3 cmol kg^{-1} (Table 3). The values decreased significantly from coastal to inland sites within the same soil layer (Fig. 10), reflecting to the pattern observed for electrical conductivity. Vertically, the forest soil Na^+ increased from the top layers to the bottom layers at each site, and the trend was most pronounced at coastal locations.

In cropland soils, the exchangeable Na^+ ranged from 0.04 to 2.0 cmol kg^{-1} (Table 3). Similar to forest soils, significant lateral differences were observed across most sites, with AG West exhibiting relatively high levels. However, these differences were less

doi:10.6342/NTU202502856

pronounced than those in forest soils, resulting in a weaker coastal–inland gradient (Fig. 9). Vertically, no significant trends within soil profiles were observed across most sites, except at AG East, where a slight increase in exchangeable Na^+ was found from surface to deeper layers.

When comparing land-use types at each site, the disparity in exchangeable Na^+ was significantly obvious at the coastal sites. AG West exhibited the largest difference, whilehere was no significant difference between forest and cropland soils at the most inland HSR site (Table 3).

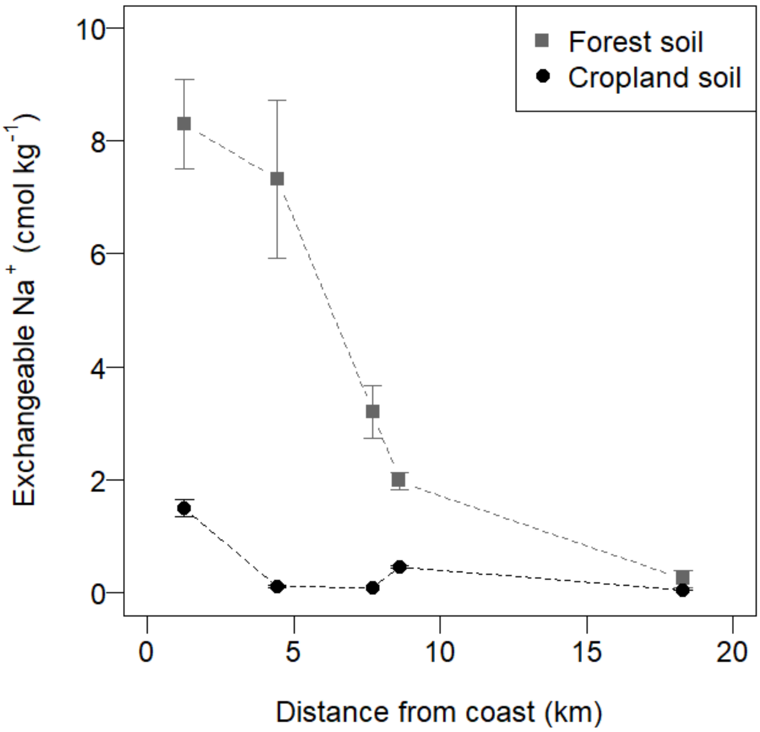

Fig. 9. Relationship between soil exchangeable Na^+ and distance from the coast to inland. Each point represents the mean exchangeable Na^+ across all soil layers at a given site. Forest soils are shown as gray squares, and cropland soils as black dots. Exchangeable Na^+ in forest soils shows a clear decreasing trend with increasing distance from the coast to inland. In contrast, cropland soils maintain consistently low levels of exchangeable Na^+, with no distinct spatial pattern—only a slight decrease away from

doi:10.6342/NTU202502856

the coast.

(2) Exchangeable Magnesium:

Exchangeable Mg^{2+} in forest soils ranges from 0.2 to 6.7 cmol kg^{-1} (Table 3). Across sites within the same soil layer, significantly higher values were observed in the inland locations such as GC and HSR, while the coastal sites showed lower and statistically similar levels. In cropland soils, exchangeable Mg^{2+} ranged from 0.1 to 1.4 cmol kg^{-1} (Table 3). A clear inland-increasing trend was only observed in the 0-20 cm layer; the remaining layers showed no significant lateral differences. Overall, forest soils displayed a clear spatial gradient of exchangeable Mg^{2+} increasing from coast to inland, whereas cropland soils showed no consistent spatial pattern (Fig. 10). Vertically, most sites showed no significant differences between layers.

When comparing land-use types, forest and cropland soils generally did not differ significantly in exchangeable Mg^{2+} content at the same site (see Table 3). The only exception was the HSR site, where forest soil had significantly higher Mg^{2+} levels than its cropland counterpart.

doi:10.6342/NTU202502856

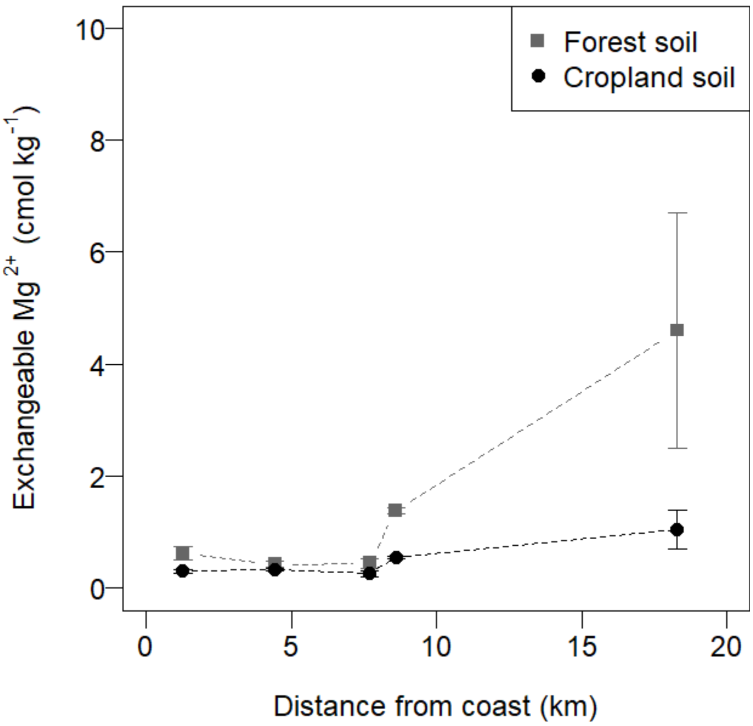

Fig. 10. Relationship between soil exchangeable Mg^{2+} and distance from the coast to inland. Each point represents the mean exchangeable Mg^{2+} across all soil layers at a given site. Forest soils are shown as gray squares, and cropland soils as black dots. Exchangeable Mg^{2+} in forest soils shows a clear increasing trend with distance inland. In contrast, cropland soils maintain consistently low exchangeable Mg^{2+} with no apparent spatial pattern.

(3) Exchangeable Calcium:

Exchangeable Ca^{2+} in forest soils ranged from 1.0 to 9.3 cmol kg^{-1} (Table 3). In the upper layers (0-20 cm and 20-40 cm), significant differences were observed among sites, showing a general trend of increasing values from coast toward inland locations (Fig. 11). In cropland soils, the pattern of exchangeable Ca^{2+} was generally similar to that of forest soils (Table 3), but both lateral and vertical trends were less distinct. Exchangeable Ca^{2+} did not vary significantly among layers at most sites in both forest and cropland soils.

doi:10.6342/NTU202502856

When comparing land-use types, exchangeable Ca^{2+} contents between forest and cropland soils were generally not significantly different at the same site (Table 3).

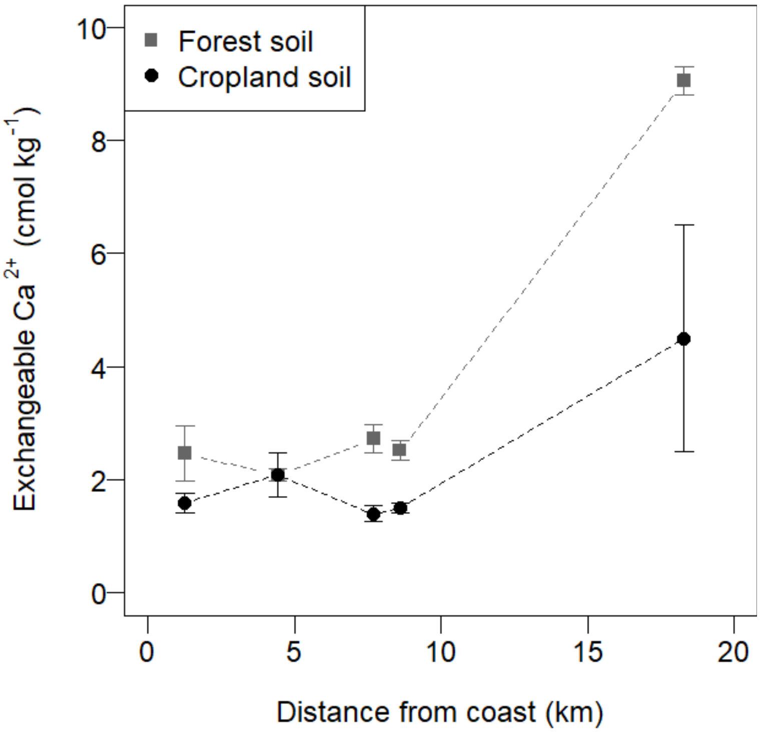

Fig. 11. Relationship between soil exchangeable Ca^{2+} and distance from the coast. Each point represents the mean exchangeable Ca^{2+} across all soil layers at a given site. Forest soils are shown as gray squares, and cropland soils as black dots. Exchangeable Ca^{2+} in forest soils shows a clear increasing trend with distance inland. Cropland soils display a similar but less pronounced pattern.

3.2.3 Exchangeable Sodium Percentage (ESP)

The mean ESP of forest soils ranges from 0.4% to 2771.5% (Table 3). A pronounced lateral trend is observed, with ESP values decreasing significantly from coastal to inland areas when comparing the same soil layers across sites. Coastal sites such as AG West and AG East exhibit extremely high ESP values, exceeding 100%,

doi:10.6342/NTU202502856

whereas the most inland site, HSR site, has the ESP values below 2%. Although lower soil layers generally exhibit higher ESP values, no statistically significant differences were observed between layers within the same site due to the overall high ESP variation in forest soils. The HSR site is an exception, with consistently low ESP in both layers, though slightly higher in the lower layer.

In cropland soils, the mean ESP ranges from 0.4% to 35.1% (Table 3). No statistically significant differences are found between the same layers across different sites, even though the GC site exhibited relatively higher ESP values compared to other sites. Vertically, there is no significant difference in ESP between layers within the same site; however, the deeper layer tends to have slightly higher values.

When comparing forest and cropland soils at the same site, ESP is significantly higher in forest soils than in cropland soils at AG West, AG East, and BG (Table 3). At GC site, no consistent differences between forest and cropland soils were observed, except in the 80–100 cm layer, where the ESP in forest soils showed significantly higher values than cropland soils. The most inland site, HSR, showed the minimal differences in the ESP values and no difference was found between forest and cropland soils.

doi:10.6342/NTU202502856

Table 3. Soil Salinity Properties of Aogu Wetland

Salinity Properties	Land Type	Depth (cm)	AG West	AG East	BG	GC	HSR
ECe (dS m^{-1})	Forest	0-20	18.2 ± 1.6 Abc	8.4 ± 3.1 Bc	4.6 ± 2.3 Ba	5.5 ± 2.5 Ba	0.3 ± 0.03 Bb
		20-40	17.2 ± 0.9 Ac	12.5 ± 5.3 ABbc	5.0 ± 1.7 BCa	5.3 ± 2.1 BCa	0.3 ± 0.02 Cb
		40-60	19.9 ± 1.3 Aabc	15.2 ± 3.1 Aabc	6.4 ± 1.8 Ba	6.2 ± 2.3 Ba	0.6 ± 0.1 Ba
		60-80	24.2 ± 2.1 Aa	22.3 ± 1.3 Aab	7.2 ± 2.1 Ba	6.6 ± 2.3 Ba	-
		80-100	23.0 ± 2.0 Aab	25.6 ± 0.2 Aa	7.5 ± 2.4 Ba	7.1 ± 2.2 Ba	-
	Cropland	0-20	0.7 ± 0.2 Ba	0.4 ± 0.02 Ba	0.2 ± 0.02 Ba	1.9 ± 0.5 Aa	0.6 ± 0.1 Ba
		20-40	0.9 ± 0.5 ABa	0.4 ± 0.1 Ba	0.2 ± 0.03 Ba	1.5 ± 0.5 Aa	0.3 ± 0.01 Bb
		40-60	1.4 ± 0.7 ABa	0.4 ± 0.05 BCa	0.3 ± 0.1 Ca	1.4 ± 0.5 Aa	0.3 ± 0.1 Cb
		60-80	1.5 ± 0.6 Aa	0.6 ± 0.1 Aa	0.2 ± 0.02 Aa	1.8 ± 1.0 Aa	-
		80-100	1.5 ± 0.4 Aa	0.8 ± 0.3 Aa	0.2 ± 0.1 Aa	1.7 ± 0.9 Aa	-
$EC_{1:5}$ (dS m^{-1})	Forest	0-20	1.6 ± 0.2 Aab	0.9 ± 0.3 ABc	0.5 ± 0.2 BCa	0.5 ± 0.2 BCa	0.03 ± 0.0 Ca
		20-40	1.5 ± 0.1 Ab	1.1 ± 0.4 Bbc	0.6 ± 0.2 Ba	0.4 ± 0.2 Ba	0.04 ± 0.01 Ba
		40-60	1.7 ± 0.1 Aab	1.5 ± 0.3 ABbc	0.9 ± 0.2 BCa	0.6 ± 0.2 CDa	0.1 ± 0.0 Da
		60-80	2.1 ± 0.2 Aa	2.1 ± 0.2 Aab	1.1 ± 0.2 Ba	0.6 ± 0.2 Ba	-
		80-100	2.0 ± 0.2 Aa	2.5 ± 0.4 ABa	1.3 ± 0.3 BCa	0.7 ± 0.2 Ca	-
	Cropland	0-20	0.1 ± 0.04 ABa	0.1± 0.0 Bc	0.04 ± 0.01 Ba	0.2 ± 0.1 Aa	0.1 ± 0.01 Ba
		20-40	0.5 ± 0.2 Aa	0.1 ± 0.01ABbc	0.1 ± 0.02 ABa	0.2 ± 0.1 ABa	0.03 ± 0.0 Bb
		40-60	0.2 ± 0.1 Aa	0.1 ± 0.0 ABCbc	0.1 ± 0.02 BCa	0.1 ± 0.1 ABa	0.03 ± 0.01 Cb
		60-80	0.2 ± 0.1 Aa	0.1 ± 0.01 Aab	0.1 ± 0.01 Aa	0.2 ± 0.1 Aa	-
		80-100	0.2 ± 0.1 Aa	0.2 ± 0.04 Aa	0.1 ± 0.01 Aa	0.2 ± 0.1 Aa	-

doi:10.6342/NTU202502856

Exchangeable Na^{+} (cmol kg^{-1})	Forest	0-20	6.7 ± 1.1 Ab	3.9 ± 1.8 ABb	2.0 ± 0.6 ABa	1.7 ± 0.8 Ba	0.1 ± 0.03 Ca
		20-40	6.3 ± 0.9 Ab	5.3 ± 2.9 Aab	2.5 ± 0.7 ABa	1.7 ± 0.6 Ba	0.2 ± 0.01 Ca
		40-60	8.5 ± 0.6 Aab	6.3 ± 1.6 ABab	3.1 ± 0.9 BCa	1.9 ± 0.7 Ca	-
		60-80	10.1 ± 0.9 Aa	11.3 ± 0.3 Aa	3.8 ± 1.1 Ba	2.1 ± 0.7 Ba	-
		80-100	9.9 ± 0.9 Aa	9.8 ± 1.6 Aa	4.6 ± 1.3 ABa	2.5 ± 0.8 Ba	-
	Cropland	0-20	1.5 ± 0.3 Aa	0.1 ± 0.03 Cab	0.1 ± 0.03 Ca	0.5 ± 0.2 Ba	0.05 ± 0.01 Ca
		20-40	1.4 ± 0.1 Aa	0.1 ± 0.04 ABab	0.1 ± 0.04 Ba	0.4 ± 0.2 ABa	0.04 ± 0.01 Ba
		40-60	1.5 ± 0.1 Aa	0.1 ± 0.05 Cb	0.1 ± 0.06 BCa	0.4 ± 0.1 ABa	-
		60-80	1.1 ± 0.3 Aa	0.2 ± 0.03 Bab	0.1 ± 0.04 Ba	0.5 ± 0.1 Aa	-
		80-100	2.0 ± 1.2 Aa	0.2 ± 0.03 BCa	0.1 ± 0.02 Ca	0.5 ± 0.2 ABa	-
Exchangeable Ca^{2+} (cmol kg^{-1})	Forest	0-20	1.0 ± 0.3 Cd	1.7 ± 0.2 BCa	2.4 ± 0.6 Ba	2.1 ± 0.6 BCa	8.8 ± 0.4 Aa
		20-40	1.9 ± 0.3 Bcd	2.3 ± 0.3 Ba	2.1 ± 0.8 Ba	2.2 ± 0.5 Ba	9.3 ± 0.4 Aa
		40-60	2.4 ± 0.2 Abc	2.2 ± 0.04 Aa	3.6 ± 0.9 Aa	2.6 ± 0.8 Aa	-
		60-80	3.2 ± 0.1 Aab	2.2 ± 0.3 Aa	2.8 ± 0.5 Aa	2.7 ± 1.1 Aa	-
		80-100	3.8 ± 0.5 Aa	2.0 ± 0.0 Aa	2.7 ± 0.3 Aa	3.0 ± 0.6 Aa	-
	Cropland	0-20	1.6 ± 0.0 Ba	1.1 ± 0.04 Ba	1.1 ± 0.2 Ba	1.8 ± 0.6 Ba	6.5 ± 0.2 Aa
		20-40	1.1 ± 0.0 Aa	1.4 ± 0.5 Aa	1.1 ± 0.2 Aa	1.4 ± 0.5 Aa	2.5 ± 1.1 Aa
		40-60	2.0 ± 0.4 Aa	2.0 ± 0.5 Aa	1.9 ± 0.8 Aa	1.3 ± 0.5 Aa	-
		60-80	1.3 ± 0.1 Aa	2.7 ± 0.8 Aa	1.4 ± 0.0 Aa	1.4 ± 0.2 Aa	-
		80-100	1.9 ± 0.2 Ba	3.2 ± 0.2 Aa	1.5 ± 0.3 Ba	1.6 ± 0.4 Ba	-
Exchangeable Mg^{2+} (cmol kg^{-1})	Forest	0-20	0.6 ± 0.2 Cab	0.5 ± 0.05 Cab	0.2 ± 0.1 Ca	1.3 ± 0.4 Ba	2.5 ± 0.1 Ab
		20-40	0.7 ± 0.2 BCab	0.4 ± 0.1 Cab	0.3 ± 0.1 Ca	1.2 ± 0.3 Ba	6.7 ± 0.5 Aa
		40-60	0.2 ± 0.1 Bb	0.3 ± 0.1 Bab	0.6 ± 0.3 Ba	1.5 ± 0.5 Aa	-

doi:10.6342/NTU202502856

		60-80	0.6 ± 0.1 Bab	0.3 ± 0.1 Bb	0.5 ± 0.1 Ba	1.4 ± 0.4 Aa	-
		80-100	1.0 ± 0.2 Aa	0.6 ± 0.1 Aa	0.6 ± 0.2 Aa	1.5 ± 0.4 Aa	-
	Cropland	0-20	0.2 ± 0.02 Ca	0.3 ± 0.1 BCa	0.4 ± 0.1 BCa	0.6 ± 0.2 Ba	1.4 ± 0.1 Aa
		20-40	0.3 ± 0.03 ABa	0.3 ± 0.04 ABa	0.1 ± 0.1 Bb	0.5 ± 0.2 ABa	0.7 ± 0.3 Aa
		40-60	0.3 ± 0.1 Aa	0.4 ± 0.04 Aa	0.3 ± 0.1 Aab	0.5 ± 0.2 Aa	-
		60-80	0.3 ± 0.01 Aa	0.3 ± 0.2 Aa	0.3 ± 0.04 Aab	0.5 ± 0.1 Aa	-
		80-100	0.4 ± 0.1 Aa	0.3 ± 0.2 Aa	0.2 ± 0.03 Ab	0.6 ± 0.2 Aa	-
ESP (%)	Forest	0-20	1025.0 ± 807.2 Aa	477.2 ± 329.0 Aa	119.2 ± 28.8 ABb	49.6 ± 22.6 Ba	0.4 ± 0.1 Cb
		20-40	2771.5 ± 1702.5 Aa	802.8 ± 520.8 ABa	111.7 ± 23.4 Bb	48.3 ± 13.9 Ba	1.7 ± 0.3 Ca
		40-60	328.6 ± 60.0 Aa	798.5 ± 295.2 Aa	530.9 ± 150.2 Aa	50.2 ± 19.0 Ba	-
		60-80	684.0 ± 223.3 ABa	1630.8 ± 507.7 Aa	297.1 ± 24.6 Ba	55.5 ± 15.9 Ca	-
		80-100	948.7 ± 228.4 Aa	891.5 ± 818.7 ABa	275.5 ± 85.6 ABa	61.5 ± 7.4 Ba	-
	Cropland	0-20	17.1 ± 3.0 ABa	4.3 ± 1.5 BCa	4.2 ± 2.4 Ca	24.9 ± 13.8 Aa	0.4 ± 0.04 Db
		20-40	23.2 ± 7.1 Aa	3.4 ± 1.9 Aa	3.9 ± 1.0 Aa	22.8 ± 15.8 Aa	1.6 ± 0.1 Aa
		40-60	18.4 ± 3.3 Aa	4.7 ± 2.8 Aa	17.8 ± 13.1 Aa	14.4 ± 3.9 Aa	-
		60-80	7.0 ± 0.3 Ba	6.9 ± 1.9 Ba	4.6 ± 1.4 Ba	35.1 ± 12.5 Aa	-
		80-100	18.0 ± 6.6 ABa	7.7 ± 1.7 Ba	9.5 ± 3.3 Ba	27.5 ± 4.8 Aa	-
Forest vs Farm independent t-test							
ECe (dS m^{-1})	-	0-20	*	NS	NS	NS	*
		20-40	*	NS	NS	NS	NS
		40-60	*	*	NS	NS	-
		60-80	*	*	NS	NS	-
		80-100	*	*	NS	NS	-

doi:10.6342/NTU202502856

$EC_{1:5}$ (dS m^{-1})	-	0-20	*	*	NS	NS	NS
		20-40	*	NS	NS	NS	NS
		40-60	*	*	NS	NS	-
		60-80	*	*	*	NS	-
		80-100	*	NS	*	NS	-
Exchangeable Na^{+} (cmol kg^{-1})	-	0-20	*	*	*	NS	NS
		20-40	*	*	*	NS	*
		40-60	*	*	*	NS	-
		60-80	*	*	*	NS	-
		80-100	*	*	*	*	-
Exchangeable Ca^{2+} (cmol kg^{-1})	-	0-20	NS	*	NS	NS	NS
		20-40	*	NS	NS	NS	*
		40-60	NS	NS	NS	NS	-
		60-80	*	NS	NS	NS	-
		80-100	NS	NS	NS	NS	-
Exchangeable Mg^{2+} (cmol kg^{-1})	-	0-20	NS	NS	NS	NS	*
		20-40	NS	NS	NS	NS	*
		40-60	NS	NS	NS	NS	-
		60-80	*	NS	NS	NS	-
		80-100	NS	NS	NS	NS	-
ESP (%)	-	0-20	*	*	*	NS	NS
		20-40	*	*	*	NS	NS
		40-60	*	*	*	NS	-
		60-80	*	*	*	NS	-

doi:10.6342/NTU202502856

80-100	*	*	*	NS	-

[a] Different uppercase letters indicate significant differences among sites within the same soil layer (post hoc comparison).

[b] Different lowercase letters indicate significant differences among soil layers within the same site (post hoc comparison).

[c] Independent t-tests were conducted to compare forest and cropland soils; results with $p < 0.05$ are labeled as *, while those with $p > 0.05$ are labeled as NS (not significant).

doi:10.6342/NTU202502856

3.2.4 Relationship between Different Salinity Indicators

Table 4 presented the Pearson correlation coefficients among different salinity indicators. The EC_e, $EC_{1:5}$, and exchangeable Na were shown to be highly correlated. ESP had a moderate correlation with EC_e, $EC_{1:5}$, and exchangeable Na, and exchangeable Ca and Mg did not show any correlation. Fig. 12 to Fig. 14 further illustrated the linear relationships between EC_e and seawater-derived cations potentially contributing to soil salinization. A significant positive correlation was observed between EC_e and sodium-related indicators, including exchangeable Na^+ and ESP. In contrast, EC_e showed no significant correlation with exchangeable Mg^{2+} or Ca^{2+}.

3.3 SEM-EDS Images

SEM-EDS images (Fig. 15-17) show higher signal intensities of seawater-related ions (Na^+, K^+, Cl^-) in forest (saline) soil than in cropland (non-saline) soil, while Mg^{2+} and Ca^{2+} levels were similar. Notably, the 20 μm zoom-in image (x900, data nor shown) did not reveal large salt particles rich in Na^+ and Cl^-, suggesting that salts are likely distributed diffusely rather than as distinct particles.

doi:10.6342/NTU202502856

Table 4. Pearson Correlation Coefficients Among Salinity Indicators

	EC_e	$EC_{1:5}$	Exch. Na^+	Exch. Mg^{2+}	Exch. Ca^{2+}	ESP
EC_e	1.00					
$EC_{1:5}$	0.97	1.00				
Exch. Na^+	0.97	0.95	1.00			
Exch. Mg^{2+}	-0.05	-0.07	-0.08	1.00		
Exch. Ca^{2+}	0.04	0.03	0.04	0.79	1.00	
ESP	0.46	0.44	0.41	-0.04	-0.05	1.00

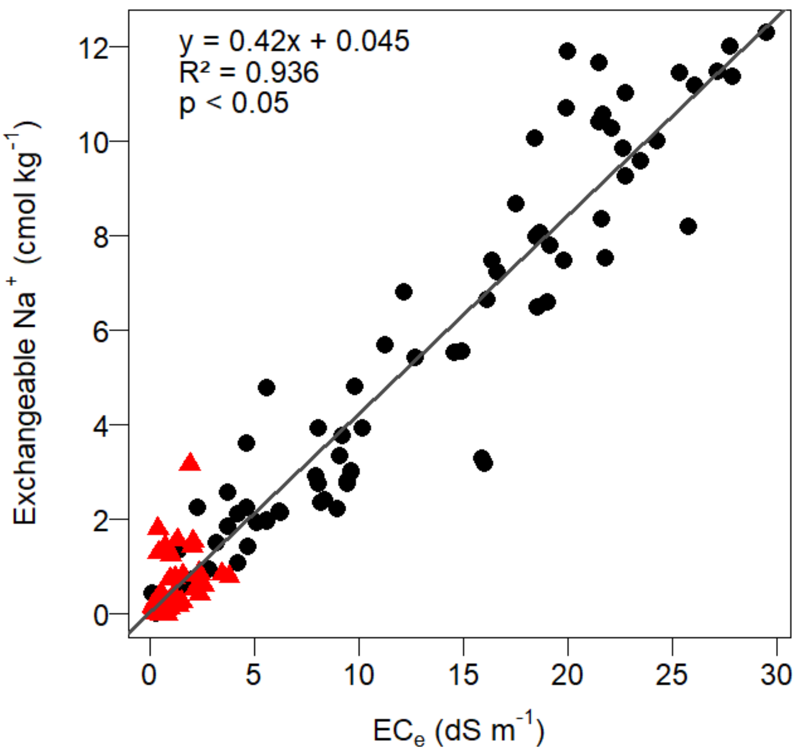

Fig. 12. Correlation between EC_e and exchangeable Na^+. Forest soil data points are shown as black dots, and cropland soils as red triangles. Exchangeable Na^+ exhibits a strong positive correlation with EC_e.

doi:10.6342/NTU202502856

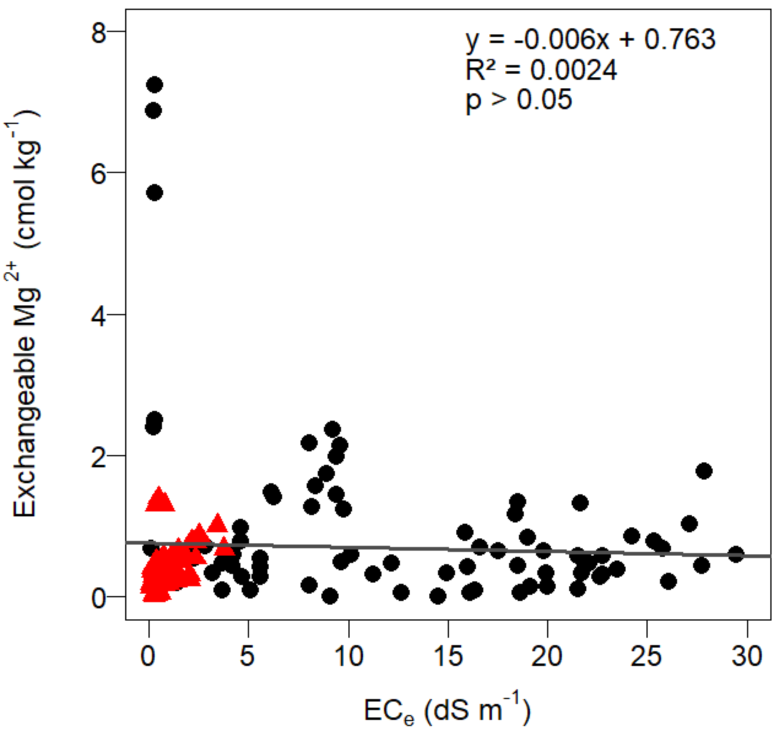

Fig. 13. Correlation between EC_e and exchangeable Mg^{2+}. Forest soil data points are shown as black dots, and cropland soils as red triangles. Exchangeable Mg^{2+} shows no significant correlation with EC_e.

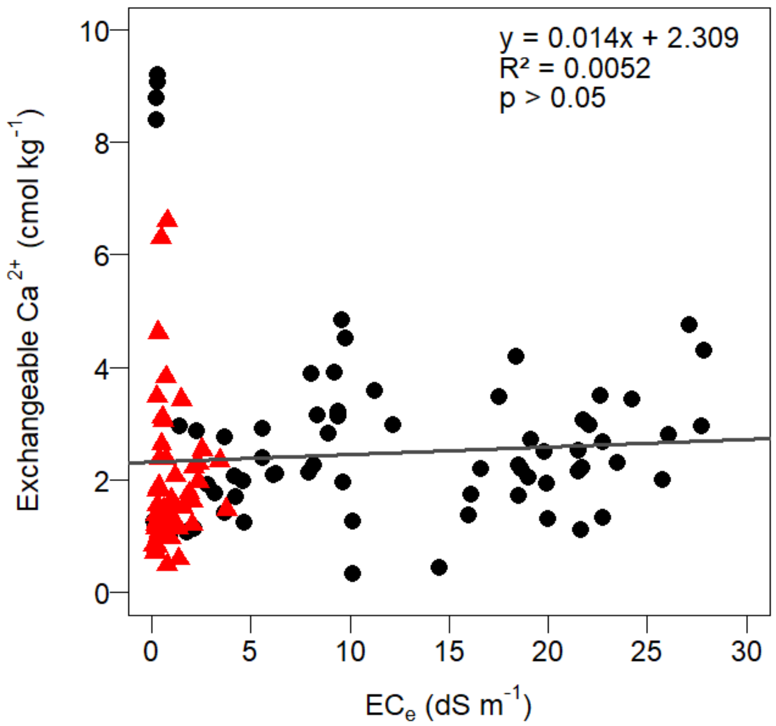

Fig. 14. Correlation between EC_e and exchangeable Ca^{2+}. Forest soil data points are shown as black dots, and cropland soils as red triangles. Exchangeable Ca^{2+} shows no significant correlation with EC_e.

doi:10.6342/NTU202502856

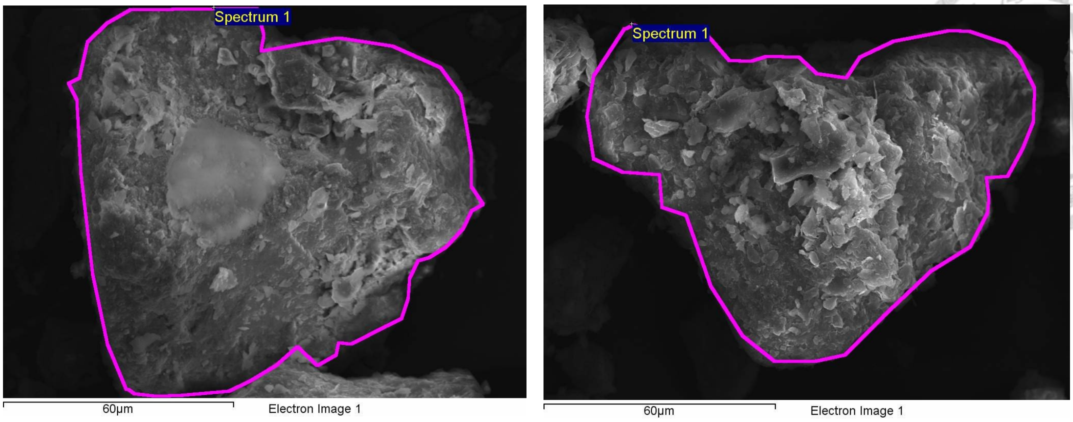

Fig 15. SEM images of soil samples (right: saline soil; left: non-saline soil). No salt crystal rich in Na^+ and Cl^- were found.

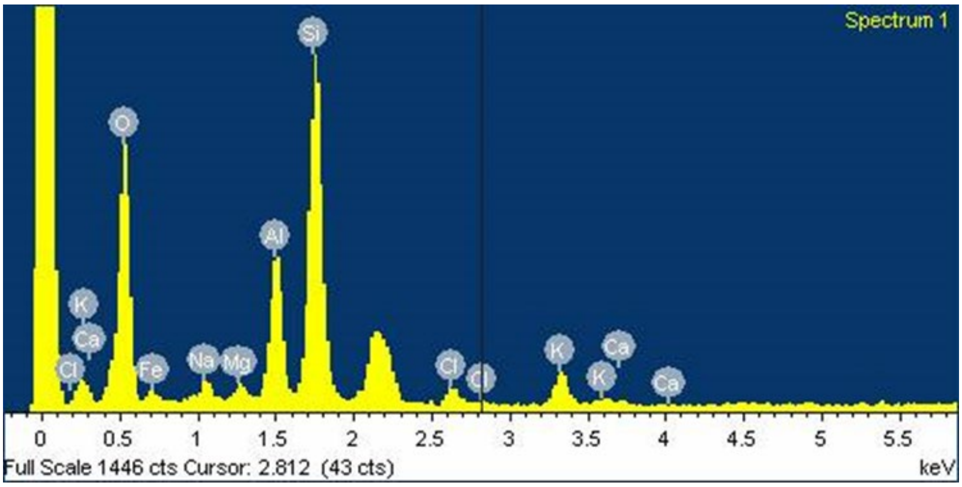

Fig 16. EDS elemental peaks of the forest soil sample (AG West). The signal intensities of seawater-related elements (Na^+, K^+, Cl^-) are notably stronger than those of most other elements, except for silicon (Si) and oxygen (O).

doi:10.6342/NTU202502856

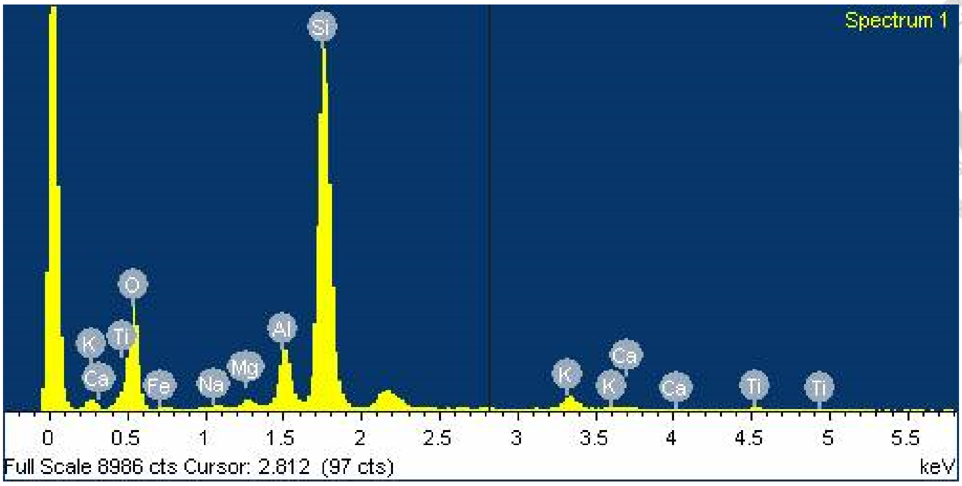

Fig. 17. EDS elemental peaks of the cropland soil sample (AG East). The signal intensities of seawater-related elements (Na^+, K^+, Cl^-) are not notably elevated compared to those of other elements.

3.4 Pot Experiment

The results of the pot experiment were summarized in Table 5. In forest soils, the maize growth generally improved with increasing distance from the coast. For example, the average maize height was only 3.9 cm in AG West Forest soil and 6.1 cm in AG East Forest soil, while it increased to 39.0 cm in BG Forest soil and 38.3 cm in HSR Forest soil (the non-saline control group).

In contrast, the maize growth in cropland soils showed less variation across sites. At the BG and AG East Farm sites, maize reached heights of 43.5 cm and 41.0 cm, respectively, and both were classified within the same statistical group. Maize grown in AG West Farm soil reached 29.6 cm, which, although lower, was still grouped statistically with the GC Forest control.

doi:10.6342/NTU202502856

Overall, the maize growth performance was better in cropland soils than in forest soils (Table 5; Fig. 18), particularly at coastal sites, particularly at AG East and AG West sites. At BG sites, no significant difference in height and only a modest difference in biomass was found between forest and cropland soils. Thus, the results of pot experiments corresponded well with soil salinity level.

Table 5. Maize Growth Performance in Soils from Each Site

Group	Height (cm)	Biomass (g)
AG West Forest	3.9 ± 2.6 C[a]	0.05 ± 0.04 D
AG West Cropland	29.6 ± 3.2 B	1.2 ± 0.4 BC
AG East Forest	6.1 ± 4.0 C	0.1 ± 0.1 D
AG East Cropland	41.0 ± 2.8 A	2.5 ± 0.4 A
BG Forest	39.0 ± 1.4 A	1.8 ± 0.1 B
BG Cropland	43.5 ± 1.3 A	3.0 ± 0.2 A
GC Forest	30.5 ± 0.7 B	0.8 ± 0.1 C
HSR Forest	38.3 ± 2.0 A	1.6 ± 0.2 B

[a] Post hoc comparisons among different sites are indicated by different uppercase letters.

doi:10.6342/NTU202502856

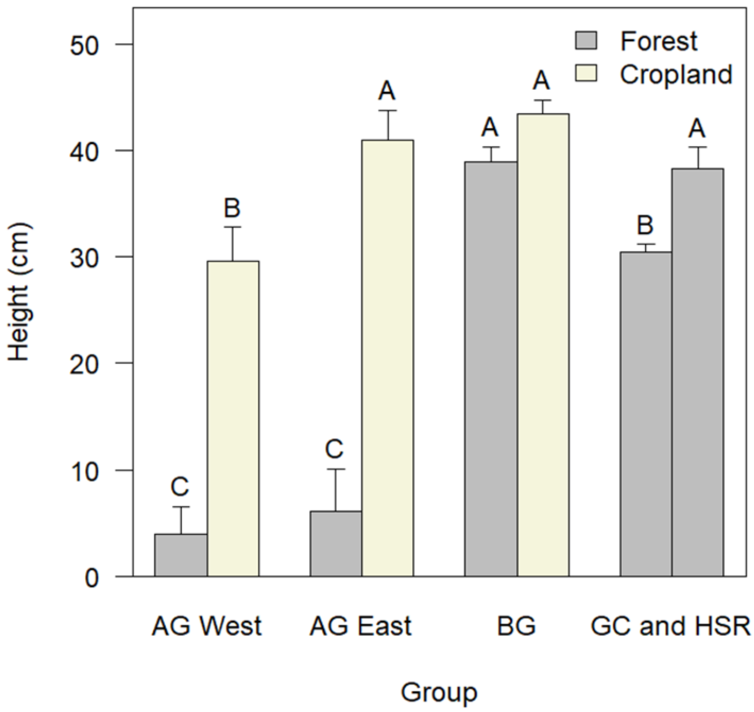

Fig. 18. Height comparison of maize grown on soils from different sites. Maize cultivated on non-saline soils (croplands and inland forests) exhibits significantly better growth performance than those grown on saline soils (coastal forest).

3.5 Ecosystem Carbon Storage

The results of ecosystem carbon storage are presented in Table 6. Among forest sites, biomass carbon storage ranges from 71.0 to 173.3 ton C ha^{-1}, with 111.8 ton C ha^{-1} as the mean carbon storage of the five sites. No significant differences are observed across most sites. However, the BG site shows a moderately higher value of 137.7 ton C ha^{-1}, while the GC site exhibits the highest biomass carbon storage at 173.3 ton C ha^{-1}, which is significantly greater than those at other sites. The annual carbon sequestration rate of biomass (after 20 years of afforestation) ranges from 3.6 to 8.7 ton C ha^{-1} yr^{-1}, with a mean of 5.6 ton C ha^{-1} yr^{-1}.

doi:10.6342/NTU202502856

The spatial pattern of carbon storage in the litter layer mirrors that of biomass carbon, with no significant differences among the AG West, AG East, and HSR sites (ranging from 2.1 to 4.9 ton C ha^{-1}). The GC site again shows the highest value at 14.8 ton C ha^{-1}. Unlike biomass carbon, the BG site also has significantly higher litter carbon storage compared to the AG West, AG East, and HSR sites.

Significant differences in soil organic carbon (SOC) storage are observed among sites in both forest and cropland soils. For both land-use types, the HSR site has the highest SOC storage: 73.4 ton C ha^{-1} in forest soil and 49.9 ton C ha^{-1} in cropland soil. The other four sites exhibit similar SOC levels, with slightly higher values at the more inland BG and GC sites (31.0-36.8 ton C ha^{-1}in forest soil; 21.6-32.1 ton C ha^{-1} in cropland soil), and relatively lower values at the coastal AG West and AG East sites (25.5-28.4 ton C ha^{-1} in forest soil; 23.4-26.8 ton C ha^{-1} in cropland soil).

When comparing SOC between forest and cropland soils within each site, no significant differences are found in most cases. Exceptions include the BG and HSR sites, where significant differences in SOC storage are observed.

By summing biomass and litter carbon stocks and adding the change in SOC resulting from land-use conversion (ΔSOC), we estimated the net ecosystem carbon storage change associated with converting cropland to forest (ΔEcosystem C). The ΔEcosystem C across the Aogu Wetland and surrounding area ranges from 72.5 to

doi:10.6342/NTU202502856

187.0 ton C ha^{-1}.

Table 6. Ecosystem C storage (ton C ha^{-1})

	AG West	AG East	BG	GC	HSR
Biomass	83.6 ± 21.1 B[a]	71.0 ± 14.4 B	137.7 ± 43.1 AB	173.3 ± 17.0 A	93.5 ± 9.8 B
Litter layer	4.9 ± 1.3 B	2.8 ± 0.5 B	12.7 ± 2.2 A	14.8 ± 1.9 A	2.1 ± 0.1 B
Soil Organic Carbon	-	-	-	-	-
Forest	28.4 ± 2.8 BC	25.5 ± 1.2 C	36.8 ± 3.1 B	31.0 ± 2.1 BC	73.4 ± 7.9A
Cropland	23.4 ± 1.8 C	26.8 ± 1.3 BC	21.6 ± 1.8 C	32.1 ± 2.1 B	49.9 ± 0.4 A
Forest vs. Cropland	$p = 0.33$	$p = 0.66$	$p = 0.04$	$p = 0.74$	$p = 0.05$
ΔSOC	+5.0	-1.3	+5.2	-1.1	+23.5
ΔEcosystem C[b]	+93.5	+72.5	+165.6	+187.0	+119.1

[a] Post hoc comparisons among different sites are indicated by different uppercase letters.

[b] ΔEcosystem C is the summation of Biomass, Litter layer, and ΔSOC.

doi:10.6342/NTU202502856

Chapter 4 Discussion

4.1 Salinization Trend

4.1.1 Soil pH

According to the results, the soil pH in the Aogu Wetland is mostly above 7, indicating that it is alkaline (Chesworth et al., 2008; McCauley et al., 2008; USDA, 2024). The high pH levels may be attributed to the limestone-derived parent material of the soil in the study area (臺灣省立中興大學農學院土壤學系，1971), as such soils typically exhibit pH values above 7.2 (Havlin et al., 2005). Consequently, the inherent alkalinity of the soil, combined with the influence of seawater intrusion, contributes to the overall alkaline condition of the Aogu Wetland soils (Arslan and Demir, 2013).

4.1.2 EC and CF

The results of EC measurements reveal significant spatial variation in soil salinity, with EC values gradually decreasing from coastal forest areas (classified as very saline) toward inland forest areas (moderately saline). Additionally, EC values are generally higher in the lower soil layers than in the upper layers, indicating a vertical distribution pattern in which salinity decreases upward through the soil profile. This vertical stratification likely reflects the influence of seawater intrusion, which increases salinity in the deeper layers (Arslan and Demir, 2013). These observations suggest that seawater intrusion occurs both laterally from the coast inland, and vertically from the bottom

doi:10.6342/NTU202502856

upward. Furthermore, comparisons of EC between forest and cropland soils at the same sites show that cropland soils consistently have significantly lower EC values than forest soils. This difference implies that the application of freshwater irrigation is effective in reducing soil salinity, thereby improving soil conditions for agricultural use (Shahid et al., 2018; Mukhopadhyay et al., 2021).

The CF between ECe and $EC_{1:5}$ determined in this study is 10.51, which exceeds the values reported in previous studies on similar soil types (Sonmez et al., 2008; Gharaibeh et al., 2021; Kargas et al, 2022). The relatively higher CF observed in the present study may be attributed to the coarser, sandier texture of the soil samples from the Aogu Wetland. In general, soils with coarser textures exhibit higher CF values due to their lower water retention capacity and weaker buffering of salt concentrations (Seo et al., 2022).

4.1.3 Exchangeable Na^+ and ESP

Exchangeable Na^+ demonstrates a pronounced spatial and vertical pattern and closely aligns with the trends observed in EC. In forest soils, exchangeable Na^+ concentrations decrease from coastal to inland sites and from deeper to shallower soil layers, suggesting that seawater intrusion occurs both laterally from the coast and vertically from the subsoil upwards. Notably, all forest soil samples—except those from the inland HSR site—exceed the recommended threshold levels for exchangeable Na^+

doi:10.6342/NTU202502856

(Hayyat et al., 2021). In contrast, exchangeable Na^+ concentrations in cropland soils remain consistently low across all sites and depths. Only at the AG West site does cropland soil exhibit slightly elevated exchangeable Na^+ levels, although they remain below critical thresholds. In most locations, forest soils contain significantly higher exchangeable Na^+ than nearby cropland soils, with the exception of the HSR site, where no significant difference is observed between land-use types. This pattern supports the notion that freshwater irrigation may play a key role in mitigating soil salinization induced by seawater intrusion (Machado and Serralheiro, 2017).

The ESP at the study sites is generally elevated (i.e., >15%), particularly in forest soils, where values frequently exceed 100%, and in some cases reach over 1000%. This extreme phenomenon is likely driven by two primary factors: elevated concentrations of exchangeable Na^+ and relatively low cation exchange capacity (CEC). The high levels of exchangeable Na^+ are attributed to seawater intrusion, which introduces substantial quantities of sodium ions into the soil profile (Ding et al., 2020). Although seawater also contains other cations that contribute to the soil's total CEC, the dominance of sodium input overwhelms their effect (Riley and Tongudai, 1967). Field observations support this interpretation; salt crust were visibly present on the soil surface at some forest sites, suggesting sodium concentrations so high that excess Na^+ could not be retained on cation exchange sites (Howari et al., 2002; Birati et al., 2025). This

doi:10.6342/NTU202502856

accumulation may lead to an overestimation of ESP, with values even exceeding 100%, particularly when free salts remain in solution rather than on exchange sites and are extracted by ammonium acetate during the determination of exchangeable cations (FAO, 2022). The FAO (2022) procedure for measuring cation exchange capacity and exchangeable bases therefore recommends removing soluble salts with 70% alcohol before ammonium acetate extraction. Alternatively, soluble salts can first be extracted using a saturated soil-water extract and then subtracted from the ammonium acetate results to obtain the true concentration of exchangeable cations. This represents an important methodological improvement that should be considered in future iterations of this research.

Last but not least, the overall low CEC further exacerbates this issue and is likely attributable to the coarse, sandy texture of the soils in the region, which limits their ability to retain cations due to high permeability and leaching losses (Ersahin et al., 2006).

4.2 Soil Salinity Drivers

Significant variation in soil salinity is observed across different parts of the Aogu Wetland and between forested and agricultural lands. The following sections explore key factors that may drive these differences.

doi:10.6342/NTU202502856

4.2.1 Irrigation

Data from multiple indicators and pot experiments consistently demonstrate that elevated soil salinity adversely affects plant growth. The disparity in salinity levels between forest and cropland soils is reflected in their differing plant performance.

A primary driver of this difference is agricultural management—particularly the use of freshwater irrigation and salt leaching, which are common strategies to mitigate soil salinization (Kirwan et al., 2025). Given the extent of seawater intrusion in the region, the removal of excess salt is essential to support healthy crop production. According to local farmers, freshwater used for irrigation is mainly sourced from the Chianan Irrigation Channel (嘉南大圳). On the other hand, according to local and nearby residents, the most coastal site, AG West, located on reclaimed land, sources its non-saline irrigation and tap water from deep groundwater wells reaching depths of up to over 100 meters. This is because shallow groundwater near the coast is more susceptible to salinization due to sea-level rise, land subsidence, and seawater intrusion, whereas deeper aquifers are less affected by these processes (環境部，2023).

Research shows that in arid regions or during dry seasons, maize fields may require 200-400 mm of irrigation water per hectare (Grassini et al., 2011). In southwestern Taiwan, which experiences distinct wet and dry seasons (中央氣象署，n.d.), this need is especially critical. The end of the dry season, typically the most water-

doi:10.6342/NTU202502856

scarce period, coincides with the optimal temperature for maize growth (許健輝等，2023), further increasing irrigation demands.

As a result, continued irrigation and effective salt leaching substantially reduce salinity in cropland soils (Shahid et al., 2018; Mukhopadhyay et al., 2021). In contrast, forest soils, being undisturbed and not subject to such practices, tend to retain higher salinity levels.

4.2.2 Evapotranspiration and Land-Use Difference

Another factor contributing to the difference in salinity levels between forest and cropland soils is the variation in evapotranspiration intensity. Forest ecosystems typically exhibit higher evapotranspiration rates than agricultural lands (Verstraeten et al., 2005; Adelana et al., 2015). The increased evapotranspiration generates an upward pull that draws water, and the dissolved salts it carries, from deeper soil layers to the surface. As water exits the soil through plant uptake or evaporation, salts are left behind, gradually accumulating and increasing soil salinity over time. In afforested areas, this process exacerbates the effects of seawater intrusion by promoting salt buildup across soil layers, leading to heightened salt stress (Adelana et al., 2015; Nordio and Fagherazzi, 2024).

Rainfall is an important factor that helps reduce soil salinity. Therefore, calculating the ET_p/Rainfall ratio, as suggested by Nordio and Fagherazzi (2024), offers a

doi:10.6342/NTU202502856

straightforward and rapid way to evaluate whether soil salinization may worsen or recover in the future. According to Yeh et al. (2008) (葉信富等，2008), the mean potential evapotranspiration (ET_p) in Chiayi is approximately 3.57 mm per day, while the mean daily rainfall, based on data from the Central Weather Administration (2024), is about 6.62 mm per day. This results in an ET_p/Rainfall ratio of 0.54, indicating that, on average, soil salinization in this region may tend to recover if seawater intrusion does not continue in the future.

However, in the specific case of the Aogu Wetland coastal forest, it is unlikely that seawater intrusion will cease, and sea level rise driven by global warming and human activity represents an additional ongoing threat. Moreover, it is important to note that the evapotranspiration rates measured at weather stations in open environments may not accurately reflect conditions in coastal forests. Forests can increase evapotranspiration compared to cropland or open areas, as discussed earlier. This difference suggests that forests may experience a higher evapotranspiration than regional averages in general (Peel et al., 2010), potentially worsen soil salinization even if rainfall remains relatively high.

4.2.3 Land Subsidence and Sea Level Rise

The southwestern coastal region of Taiwan is primarily supported by agriculture and aquaculture industries. However, the long-term over-extraction of groundwater for

doi:10.6342/NTU202502856

irrigation and fish farming has led to significant land subsidence and a relative rise in sea level, thereby exacerbating seawater intrusion and soil salinization. According to data from the Water Resources Agency, Ministry of Economic Affairs, the cumulative land subsidence in Dongshi Township, Chiayi County, between 1991 and 2022 ranged from 90 to 140 cm. Over the past three decades, Dongshi Township has repeatedly recorded the highest annual subsidence rate in Chiayi County, with a peak rate of 8.7 cm per year (水利署，2023). In addition, according to groundwater monitoring data from the Ministry of Environment (2023), electrical conductivity (EC) values measured at several sampling sites in Kouhu Township (Yunlin County), Dongshi Township and Budai Township (Chiayi County), near the Aogu Wetland, range from approximately 1,110 to 47,100 μmhos cm^{-1} (1.1-47.1 dS m^{-1}). In general, the standard EC threshold for irrigation water is 0.75 mS cm^{-1} (0.75 dS m^{-1}); values exceeding this indicate an excessive concentration of ions, suggesting salinization (林經偉, 2014). Therefore, based on the aforementioned data, even the lowest EC value recorded in the groundwater near the Aogu Wetland surpasses the upper limit of acceptable EC for irrigation water. This suggests that the region's groundwater is already facing severe soil salinization and seawater intrusion (Arslan et al., 2013).

4.3 Evidence of the Maize Pot Experiment

Maize growth showed a clear negative relationship with soil salinity: plants grew

doi:10.6342/NTU202502856

better inland where soil EC was lower (Fig. 19; Machado and Serralheiro, 2017). Within each site, maize in cropland consistently outperformed that in adjacent forest plots in height and biomass. BG Cropland and AG East Cropland even exceeded the growth seen in non-salinized control plots, indicating minimal salinity stress (Ding et al., 2020). BG Forest, though lower in growth, was similar to HSR Forest, suggesting little salinity impact.

AG West Cropland had intermediate growth, likely reflecting moderate seawater intrusion mitigated by irrigation and salt leaching (Wang et al., 2017; Khosla et al., 1979). Furthermore, AG West and AG East Forest plots had the poorest maize growth, reflecting severe salinization effects in unmanaged coastal wetlands, likely exceeding maize’s salt tolerance (Maas et al., 1983). However, cropland plots in these areas showed better growth, highlighting the benefits of active soil management.

doi:10.6342/NTU202502856

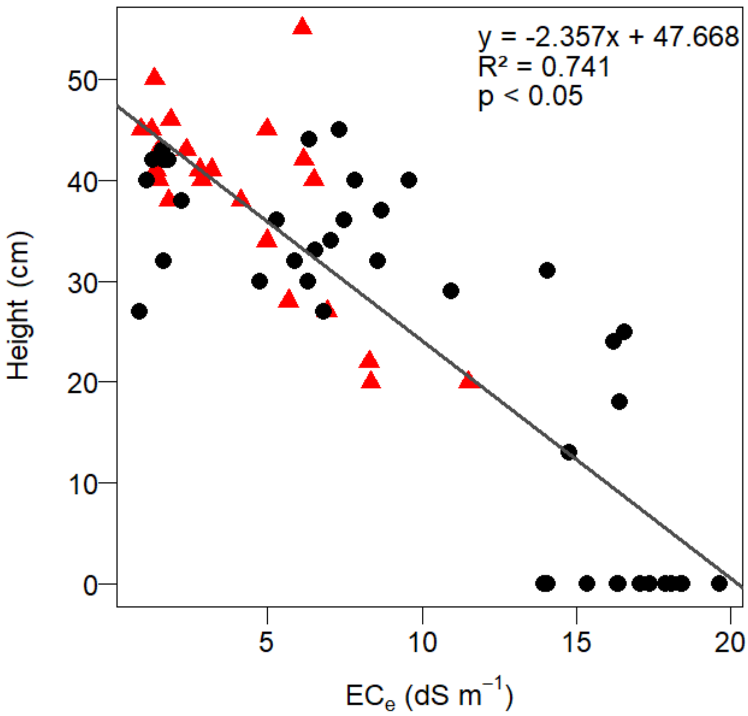

Fig. 19. Correlation between soil EC and maize height. Forest soil data points are shown as black dots; cropland soil data points are shown as red triangles. A negative correlation is observed between soil EC and maize height, suggesting that elevated soil salinity adversely affects crop growth performance.

4.4 Ecosystem Carbon Storage

4.4.1 Tree Biomass and Litter Layer

Carbon storage in tree biomass across the different sites showed no significant variation, suggesting that soil salinity differences in the Aogu Wetland coastal forest do not markedly affect tree biomass or litter layer carbon (Table 6). This consistency is likely attributable to the widespread use of salt-tolerant species such as *Melaleuca cajuputi*, *Corymbia citriodora*, and *Casuarina equisetifolia*, which dominate the afforestation sites (Sun and Dickinson, 1995; Tomar and Gupta, 2002; Ribeiro-Barros et

doi:10.6342/NTU202502856

al., 2022; Huynh et al., 2023). Only the HSR site includes *Swietenia macrophylla*, a species less adapted to saline conditions. The relatively uniform growth performance across sites implies that species selection tailored to local environmental stressors, such as salinity, plays a critical role in maintaining stable carbon storage in afforested ecosystems. This further suggests that, with appropriate species selection, high soil salinity does not necessarily compromise tree growth or carbon sequestration capacity. However, it is worth noting that the coastal forest in Aogu Wetland exhibits a relatively high carbon sequestration rate, ranging from approximately 3.6 to 8.7 tons C ha^{-1} yr^{-1}, which is an unusually high value compared to similar environments. This may be attributed to the dominance of fast-growing tree species (Doran and Turnbull, 1997; Ghorab et al., 2017) used in afforestation, which likely enabled the trees to reach their species-specific upper limit of carbon sequestration under the given site conditions.

4.4.2 Soil Organic Carbon

The results from the belowground analysis indicate that the soil organic carbon (SOC, Table 6) concentrations in forest plots were similar across areas with different levels of salinization. Moreover, the SOC concentrations in forest soils were generally higher than those in agricultural soils (though two plots showed no statistically significant difference). However, despite differences in land use, the similarity—or occasionally lower values—of forest soil bulk density compared to cropland soils

doi:10.6342/NTU202502856

resulted in no substantial difference in estimated soil carbon storage per hectare between forests and croplands. This suggests that forest soil organic carbon storage is not necessarily higher than that of agricultural land. Only in the HSR site was the soil carbon storage noticeably higher, likely due to the clayey soil texture in that area, which tends to retain more organic matter (Schweizer et al., 2021).

These findings suggest that, in terms of soil organic carbon alone, converting agricultural land to forest does not lead to a substantial increase in total soil carbon storage. Several factors may contribute to this phenomenon. It could be due to the relatively short time since afforestation, meaning that SOC accumulation has not yet reached a stable state (Xing et al., 2023); soil compaction resulting from prior agricultural use (Shete et al., 2016); intrinsic soil properties that hinder litter decomposition—such as high alkalinity slowing down carbon accumulation in litter (Yang et al., 2019); the litter of the planted species is relatively hard to decompose (Dutta and Agrawal, 2001; Cunha et al., 2019; Teixeira et al., 2020; Xu et al. 2022); or even cropland management practices like mulching and conservation tillage, which contribute to SOC retention (Amoakwah et al., 2022; Xiao et al., 2024).

Nonetheless, this does not imply that converting cropland to forest is meaningless in terms of ecosystem carbon storage. When carbon stored in the forest's biomass and litter layer is also considered, the overall ecosystem carbon storage potential

doi:10.6342/NTU202502856

significantly increases after conversion from cropland to forest (Table 6). Given that cropland, especially non-salinized soils, contributes to food production, while forests provide substantially higher carbon storage, balancing these trade-offs will be a critical challenge for future coastal land management.

4.5 Trade-off between Ecosystem Carbon Storage and Usable Cropland

Balancing ecosystem services and agricultural productivity in coastal saline soils presents a significant challenge. On one hand, proactive agricultural measures, such as irrigation and salt leaching, can substantially reduce soil salinity in croplands compared to afforested soils that remain unmanaged. These interventions can lower salinity to minimal levels or even eliminate it, making saline soils more viable for crop production. However, this agricultural gain comes at the expense of valuable ecosystem services provided by coastal afforestation, including biodiversity enhancement, long-term carbon sequestration, soil stabilization, and recreational or aesthetic value (Barry et al., 2014; Paul et al., 2016; Wang and Li, 2022).

Yet, agricultural interventions are not without limitations. Tilling saline soils may bring deeper salts to the surface, intensifying salinity stress. Overuse of groundwater for irrigation may worsen secondary salinization and even lower the groundwater table, increasing the risk of seawater intrusion (Kirwan et al., 2025). Furthermore, widely used soil amendments, such as gypsum or other liming materials rich in calcium and

doi:10.6342/NTU202502856

magnesium, aim to increase exchangeable Ca^{2+} to displace excess Na^{+}. However, the displaced sodium may leach into adjacent freshwater bodies, raising environmental concerns. While such amendments help alleviate sodium-related issues, they may simultaneously raise total soil salinity (Cox et al., 2018).

To navigate this trade-off, some have proposed compromise solutions such as agroforestry systems or cultivating salt-tolerant crop varieties. These approaches may temporarily sustain land use and food production in saline-prone coastal zones. Nevertheless, as climate change accelerates and sea levels continue to rise, even these strategies may not suffice. The long-term viability of agricultural use in these regions could be undermined by intensifying salinization and seawater intrusion, potentially forcing the eventual abandonment of vulnerable coastal lands (Kirwan et al., 2025). In such scenarios, nature may reclaim these areas, converting them into ecosystems adapted to saline conditions—a process that aligns with afforestation using salt-tolerant tree species.

This dilemma underscores a deeper question for land managers and policymakers: should we prioritize agricultural expansion to meet urgent food security needs, or invest in coastal afforestation to maximize long-term ecological benefits? The resolution will ultimately require a context-specific, adaptive strategy that balances short-term human demands with long-term ecosystem resilience and sustainability (Fig. 20).

doi:10.6342/NTU202502856

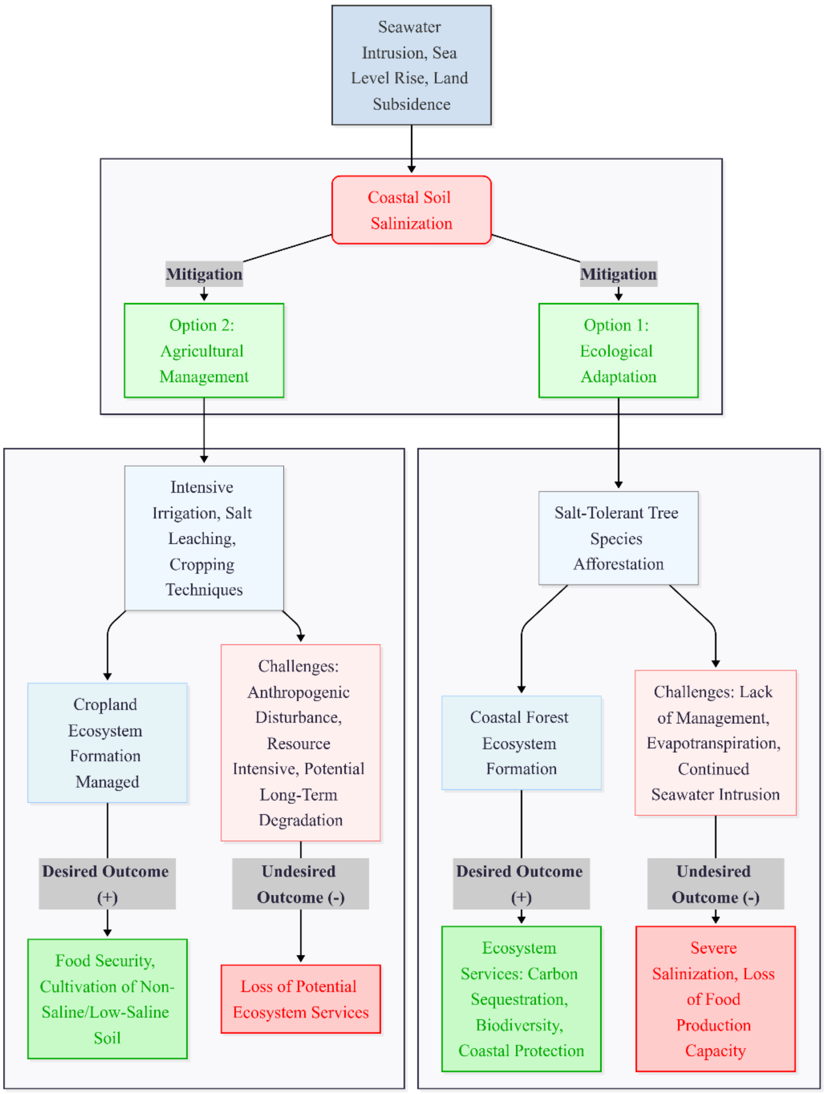

Fig. 20 Trade-offs between soil salinization and ecosystem carbon sequestration. Two distinct mitigation pathways lead to different outcomes, each associated with its own set of benefits and drawbacks.

doi:10.6342/NTU202502856

Chapter 5 Conclusion

This study investigated the current soil salinty and ecosystem carbon storage of coastal forests and croplands in the Aogu Wetland, located along the southwestern coast of Taiwan, by collecting soil samples and analyzing chemical properties related to salinity and alkalinity. The study also aimed to assess the outcomes after 20 years of afforestation in the region.

The results showed that soils in the coastal forest of Aogu Wetland and nearby region have been affected by seawater intrusion and show clear signs of salinization and alkalization. Electrical conductivity (ECe) values reached as high as 25.6 dS m^{-1}, with salinity increasing closer to the coastline and with soil depth. This indicates that seawater intrusion progresses upward from deeper layers and inland from the coast. Furthermore, other contributing factors to forest soil salinization include land subsidence, high evapotranspiration from trees, and a lack of human intervention. On the other hand, cropland soils exhibited signs of alkalization, likely influenced by the underlying limestone parent material. The soils in croplands were low or free of salinity, which suggests that soil salinization can be efficiently prevented by human management practices such as irrigation and salt leaching. Yet the coastal and deeper layers of cropland soils still showed higher salinity indices than inland and surface layers, showing that cropland soils, although managed, are still faced with the threat of

doi:10.6342/NTU202502856

continued seawater intrusion. A pot experiment on maize also confirmed that salinized forest soils in Aogu Wetland significantly suppressed plant growth, whereas corn in cropland soil did not experience growth inhibition.

In terms of ecosystem carbon storage, afforested lands planted with salt-tolerant species such as *Corymbia citriodora*, *Melaleuca cajuputi*, and *Casuarina equisetifolia* maintained relatively healthy growth despite varying degrees of soil salinity across plots. The biomass carbon storage from trees reached an average of approximately 111.8 ton C ha^{-1}, with annual carbon sequestration rates of around 5.6 ton C ha^{-1} yr^{-1}. This is a relatively high rate, and is likely due to the use of fast-growing tree species approaching their carbon uptake potential. Litter accumulation was also high in carbon storage. For soil organic carbon, there was no difference between forests and croplands, both of which contained approximately 20-30 ton C ha^{-1}. This is likely because forest soils tend to have higher organic carbon concentrations but lower bulk density, whereas cropland soils generally exhibit lower organic carbon concentrations but higher bulk density. These results suggest that the coastal forest ecosystem of Aogu Wetland reserves more carbon than cropland, mainly owing to the contribution of tree biomass and litter layer.

In summary, both afforestation and agriculture have their respective advantages and challenges in soil salinization control. Afforestation can enhance carbon

doi:10.6342/NTU202502856

sequestration and provide ecosystem services such as biodiversity conservation but, without good soil management, can be beset by severe salinization due to seawater intrusion. On the contrary, continued agriculture with appropriate land management can prevent salinization and secure food production but may sacrifice ecosystem services offered by forests. This trade-off highlights a critical issue that future land managers must carefully consider when developing coastal land use strategies.

doi:10.6342/NTU202502856

References

中央氣象署。(2021)。*氣候月平均*。行政院交通部中央氣象署。查詢日期：2024/3/19，取自：https://www.cwa.gov.tw/V8/C/C/Statistics/monthlymean.html

中央氣象署。(n.d.)。*臺灣分區雨量的季節氣候特徵*。行政院交通部中央氣象署。查詢日期：2025/7/9，取自：https://www.cwa.gov.tw/Data/service/hottopic/14277057430.pdf

中央氣象署。(2024)。*每日雨量*。行政院交通部中央氣象署。查詢日期：2025/7/8，取自：https://www.cwa.gov.tw/V8/C/D/DailyPrecipitation.html

水利署。(2023)。*地層下陷監測資訊整合服務系統*。行政院經濟部水利署。查詢日期：2023/11/14，取自：https://landsubsidence.wra.gov.tw/water_new/SubsidenceOverview/SubIndex/10010

王百祿、楊柏椿、張玉鑽、姚財寶。(1984)。鹽性鈉土淋洗之研究。*臺灣糖業研究所研究彙報，105*，13-24。

吳以健。(2020)。*氣候變遷與氣候智慧型水稻生產之研究* (博士論文)。國立臺灣大學農藝學系。臺北。

林業及自然保育署。(2018)。*台灣山林悠遊網 鰲鼓濕地森林園區*。行政院農業部林業及自然保育署。查詢日期：2025/7/9，取自：https://recreation.forest.gov.tw/Forest/FP?typ_id=05001

林經偉。(2014)。農業灌溉水之認識與應用管理。*臺南區農業專訊*，88，12-15。

許健輝、張翊庭、黃蕙萱、劉滄棽、郭鴻裕。(2023)。利用地理資訊系統進行灌溉用水情境分析--以轉作玉米為例。*技術服務，34*，18-22。

農業試驗所。(2023)。台灣土壤資源與農地土地覆圖資瀏覽查詢系統。行政院農業部農業試驗所。查詢日期：2023/9/29，取自：http://soilsurvey.tari.gov.tw/SOA/index.aspx

doi:10.6342/NTU202502856

葉信富、李振詰、陳忠偉、張格綸。(2008)。評估蒸發皿係數以推估台灣南部地區蒸發散量之研究。*農業工程學報*，*54*，27-35。

楊純明。(2013)。氣候智能型農業生產—從環境親和調適評估機會與挑戰。*作物、環境與生物資訊*，*10*，217-228。查詢日期：2025/7/9，取自：https://scholars.tari.gov.tw/handle/123456789/3411

嘉義市政府。(2001)。*嘉義市觀光發展整體規劃：第二篇 現況分析，第一章 基地環境分* (頁2-1-2-13)。查詢日期：2025/7/9，取自：https://icmp-ws.chiayi.gov.tw/Download.ashx?u=LzAwMS9VcGxvYWQvMzk5L1JlbEZpbGUvOTY2Ni8zNzgzMzgvMjAwOTAyMDUxNzQ1MDg0LnBkZg%3d%3d&n=MjAwOTAyMDUxNzQ1MDg0LnBkZg%3d%3d

臺灣省立中興大學農學院土壤學系。(1971)。*嘉義縣土壤調查報告*。農業部農業試驗所土壤資料供應查詢平台。查詢日期：2025/7/9，取自：https://tssurgo.tari.gov.tw/Tssurgo/Search/Detail?ID=20161121122200

環境部。(2023)。*全國環境水質監測資訊網*。行政院環境部。查詢日期：2023/11/15，取自：https://wq.moenv.gov.tw/EWQP/zh/ConService/DownLoad/HistoryData.aspx

魏子穎。(2024)。*以物理分餾與穩定同位素分析檢視臺灣平地造林之土壤有機碳動態* (碩士論文)。國立臺灣大學森林環境暨資源學系。臺北。

Abd El-Hamid, H. T., Alshehri, F., El-Zeiny, A. M., and Nour-Eldin, H. (2023). Remote sensing and statistical analyses for exploration and prediction of soil salinity in a vulnerable area to seawater intrusion. *Marine Pollution Bulletin*, *187*, 114555.

Adelana, S. M., Dresel, P. E., Hekmeijer, P., Zydor, H., Webb, J. A., Reynolds, M., and Ryan, M. (2015). A comparison of streamflow, salt and water balances in adjacent

doi:10.6342/NTU202502856

cropland and forest catchments in south-western Victoria, Australia. *Hydrological Processes*, *29*, 1630-1643.

Alfarrah, N., and Walraevens, K. (2018). Groundwater overexploitation and seawater intrusion in coastal areas of arid and semi-arid regions. *Water*, *10*, 143.

Amoakwah, E., Lucas, S. T., Didenko, N. A., Rahman, M. A., and Islam, K. R. (2022). Impact of deforestation and temporal land-use change on soil organic carbon storage, quality, and lability. *PLoS One*, *17*, e0263205.

Ardón, M., Helton, A. M., and Bernhardt, E. S. (2018). Salinity effects on greenhouse gas emissions from wetland soils are contingent upon hydrologic setting: a microcosm experiment. *Biogeochemistry*, *140*, 217-232.

Arslan, H., and Demir, Y. (2013). Impacts of seawater intrusion on soil salinity and alkalinity in Bafra Plain, Turkey. *Environmental Monitoring and Assessment*, *185*, 1027-1040.

Barbier, E. B. (2019). The value of coastal wetland ecosystem services. In G. M. E. Perillo, E. Wolanski, D. R. Cahoon, and C. S. Hopkinson (Eds.), *Coastal Wetlands* (pp. 947–964). Elsevier. Amsterdam, Netherlands.

Barry, L. E., Yao, R. T., Harrison, D. R., Paragahawewa, U. H., and Pannell, D. J. (2014). Enhancing ecosystem services through afforestation: How policy can help. *Land Use Policy*, 39, 135-145.

doi:10.6342/NTU202502856

Birati, S., Amanipoor, H., and Battaleb-Looie, S. (2025). Investigation of the impact of seawater intrusion on the agricultural land quality along river margins. *Applied Water Science*, 15, 1-21.

Bronick, C. J., and Lal, R. (2005). Soil structure and management: a review. *Geoderma*, *124*, 3-22.

Seo, B. S., Jeong, Y. J., Baek, N. R., Park, H. J., Yang, H. I., Park, S. I., and Choi, W. J. (2022). Soil texture affects the conversion factor of electrical conductivity from 1:5 soil-water to saturated paste extracts. *Pedosphere*, *32*, 905-915.

Burt, C. M., and Isbell, B. (2005). Leaching of accumulated soil salinity under drip irrigation. *Transactions of the ASAE*, *48*, 2115-2121.

Cantelon, J. A., Guimond, J. A., Robinson, C. E., Michael, H. A., and Kurylyk, B. L. (2022). Vertical saltwater intrusion in coastal aquifers driven by episodic flooding: A review. *Water Resources Research*, *58*, e2022WR032614.

Cazenave, A., and Cozannet, G. L. (2013). Sea level rise and its coastal impacts. *Earth's Future*, *2*, 15-34.

Chesworth, W., Macías Vázquez, F., and Camps Arbestain, M. (2008). Alkaline soils. In W. Chesworth (Ed.), *Encyclopedia of Earth Sciences Series* (pp. 37-39). Springer. Dordrecht, Netherlands.

Cheng, C. H., Huang, Y. H., Menyailo, O. V., and Chen, C. T. (2016). Stand

doi:10.6342/NTU202502856

development and aboveground biomass carbon accumulation with cropland afforestation in Taiwan. *Taiwan Journal of Forest Science*, 31, 105-118.

Chmura, G. L., Anisfeld, S. C., Cahoon, D. R., and Lynch, J. C. (2003). Global carbon sequestration in tidal, saline wetland soils. *Global Biogeochemical Cycles*, *17*, 1111.

Cox, C., Jin, L., Ganjegunte, G., Borrok, D., Lougheed, V., and Ma, L. (2018). Soil quality changes due to flood irrigation in agricultural fields along the Rio Grande in western Texas. *Applied Geochemistry*, *90*, 87-100.

Cunha, G. M., Gama-Rodrigues, A. C., Gama-Rodrigues, E. F., and Moreira, G. R. (2019). Nutrient cycling in Corymbia citriodora in the State of Rio de Janeiro, Brazil. *Floresta e Ambiente*, *26*, e20170204.

Curtin, D., Steppuhn, H., and Selles, F. (1994). Effects of magnesium on cation selectivity and structural stability of sodic soils. *Soil Science Society of America Journal*, *58*, 730-737.

Davis, J. A., and Froend, R. J. W. E. (1999). Loss and degradation of wetlands in southwestern Australia: underlying causes, consequences and solutions. *Wetlands Ecology and Management*, *7*, 13-23.

Ding, Z., Koriem, M. A., Ibrahim, S. M., Antar, A. S., Ewis, M. A., He, Z., and Kheir, A. M. (2020). Seawater intrusion impacts on groundwater and soil quality in the

doi:10.6342/NTU202502856

northern part of the Nile Delta, Egypt. *Environmental Earth Sciences*, *79*, 1-11.

Dong, X., Wang, J., Zhang, X., Dang, H., Singh, B. P., Liu, X., and Sun, H. (2022). Long-term saline water irrigation decreased soil organic carbon and inorganic carbon contents. *Agricultural Water Management*, *270*, 107760.

Doran, J. C., and Turnbull, J. W. (Eds.). (1997). *Australian trees and shrubs: Species for land rehabilitation and farm planting in the tropics* (p. 314). Australian Centre for International Agricultural Research (ACIAR).

Dutta, R. K., and Agrawal, M. (2001). Litterfall, litter decomposition and nutrient release in five exotic plant species planted on coal mine spoils. *Pedobiologia*, *45*, 298-312.

El-Juhany, L. I., Aref, I. M., and El-Wakeel, A. O. (2002). Evaluation of above-ground biomass and stem volume of three Casuarina species grown in the central region of Saudi Arabia. *Emirates Journal of Agricultural Sciences*, *14*, 8-13.

El Shinawi, A., Kuriqi, A., Zelenakova, M., Vranayova, Z., and Abd-Elaty, I. (2022). Land subsidence and environmental threats in coastal aquifers under sea level rise and over-pumping stress. *Journal of Hydrology*, *608*, 127607.

Ersahin, S., Gunal, H., Kutlu, T., Yetgin, B., and Coban, S. (2006). Estimating specific surface area and cation exchange capacity in soils using fractal dimension of particle-size distribution. *Geoderma*, *136*, 588-597.

doi:10.6342/NTU202502856

Eswar, D., Karuppusamy, R., and Chellamuthu, S. (2021). Drivers of soil salinity and their correlation with climate change. *Current Opinion in Environmental Sustainability*, *50*, 310-318.

Food and Agriculture Organization of the United Nations. (2022). *Standard operating procedure for cation exchange capacity and exchangeable bases: 1N ammonium acetate, pH 7.0 method*. FAO. Rome, Italy.

Freibauer, A., Rounsevell, M. D., Smith, P., and Verhagen, J. (2004). Carbon sequestration in the agricultural soils of Europe. *Geoderma*, *122*, 1-23.

Gharaibeh, M. A., Albalasmeh, A. A., and El Hanandeh, A. (2021). Estimation of saturated paste electrical conductivity using three modelling approaches: Traditional dilution extracts; saturation percentage and artificial neural networks. *Catena*, *200*, 105141.

Ghorab, S. A., Ismail, M. F., and Abd El-Lah, S. A. (2017). Growth rate, basal area and volume of Corymbia citriodora and Cupressus sempervirens irrigated with treated wastewater at Serabium Forest. *Egyptian Journal of Agricultural Research*, *95*, 1145-1157.

Gibson, N., McNulty, S., Miller, C., Gavazzi, M., Worley, E., Keesee, D., and Hollinger, D. (2021). *Identification, mitigation, and adaptation to salinization on working lands in the US Southeast*. Forest Service, U.S. Department of Agriculture,

doi:10.6342/NTU202502856

Southern Research Station.

Grassini, P., Yang, H., Irmak, S., Thorburn, J., Burr, C., and Cassman, K. G. (2011). High-yield irrigated maize in the Western US Corn Belt: II. Irrigation management and crop water productivity. *Field Crops Research*, *120*, 133-141.

Groenendyk, D. G., Ferre, T. P., Thorp, K. R., and Rice, A. K. (2015). Hydrologic-process-based soil texture classifications for improved visualization of landscape function. *PloS one*, *10*, e0131299.

Hailegnaw, N. S., Bayabil, H. K., Li, Y. C., and Gao, B. (2024). Seawater flooding of calcareous soils: Implications for trace and alkaline metals mobility. *Science of The Total Environment*, *927*, 172210.

Hamed, M. H., and Khalafallh, M. Y. (2017). Available nutrients and some soil properties of El-Qasr soils, El-Dakhla Oasis, Egypt. *International Journal of Environment, Agriculture and Biotechnology*, *2*, 239023.

Havlin, J. L., Beaton, J. D., Tisdale, S. L., and Nelson, W. L. (2005). Chapter 3 Soil acidity and alkalinity. In *Soil fertility and fertilizers: An introduction to nutrient management* (pp. 45-96). Pearson. Upper Saddle River, NJ, USA.

Haywood, B. J., Hayes, M. P., White, J. R., and Cook, R. L. (2020). Potential fate of wetland soil carbon in a deltaic coastal wetland subjected to high relative sea level rise. *Science of the Total Environment*, *711*, 135185.

doi:10.6342/NTU202502856

Hayyat, M. U., Nawaz, R., Siddiq, Z., Shakoor, M. B., Mushtaq, M., Ahmad, S. R., Ali, S., Hussain, A., Irshad, M. A., Alsahli, A. A., and Alyemeni, M. N. (2021). Investigation of lithium application and effect of organic matter on soil health. *Sustainability*, *13*, 1705.

Herbert, E. R., Boon, P., Burgin, A. J., Neubauer, S. C., Franklin, R. B., Ardón, M., Hopfensperger, K. N., Lamers, L. P. M., and Gell, P. (2015). A global perspective on wetland salinization: ecological consequences of a growing threat to freshwater wetlands. *Ecosphere*, *6*, 206.

Howari, F. M., Goodell, P. C., and Miyamoto, S. (2002). Spectral properties of salt crusts formed on saline soils. *Journal of Environmental Quality*, *31*, 1453-1461.

Huynh, T., Lee, D. J., Lewis, T., and Applegate, G. (2023). Effects of site characteristics and stand management on biomass and carbon sequestration in spotted gum (Corymbia citriodora subsp. variegata) plantations. *Forest Ecology and Management*, *529*, 120725.

Iqbal, V., Velmurugan, A., Balaji, S., and Swarnan, T. P. (2018). Effect of Seawater intrusion on soil and water quality parameter in vulnerable area of South Andaman Island, India. *Journal of the Andaman Science Association*, *23*, 119-123.

Intergovernmental Panel on Climate Change (IPCC). (2006). *2006 IPCC guidelines for national greenhouse gas inventories. Volume 4: Agriculture, forestry and other land*

doi:10.6342/NTU202502856

use. Institute for Global Environmental Strategies (IGES). Hayama, Japan. https://www.ipcc-nggip.iges.or.jp/public/2006gl/vol4.html

Intergovernmental Panel on Climate Change (IPCC). (2023). *Climate change 2023: Synthesis report. Contribution of the Intergovernmental Panel on Climate Change*. Cambridge University Press. Cambridge, United Kingdom. https://www.ipcc.ch/report/ar6/syr/

Kargas, G., Londra, P., and Sotirakoglou, K. (2022). The Effect of Soil Texture on the Conversion Factor of 1:5 Soil/Water Extract Electrical Conductivity (EC1:5) to Soil Saturated Paste Extract Electrical Conductivity (ECe). *Water*, *14*, 642.

Khanom, T. (2016). Effect of salinity on food security in the context of interior coast of Bangladesh. *Ocean & Coastal Management*, *130*, 205-212.

Khorsandi, F., and Yazdi, F. A. (2011). Estimation of saturated paste extracts' electrical conductivity from 1: 5 soil/water suspension and gypsum. *Communications in Soil Science and Plant Analysis*, *42*, 315-321.

Khosla, B. K., Gupta, R. K., and Abrol, I. P. (1979). Salt leaching and the effect of gypsum application in a saline-sodic soil. *Agricultural Water Management*, *2*, 193-202.

Kim, J., Kang, Y., Kim, D., Son, S., and Kim, E. J. (2024). Carbon storage and sequestration analysis by urban park grid using i-tree eco and drone-based

doi:10.6342/NTU202502856

modeling. *Forests*, *15*, 683.

Kirwan, M. L., Michael, H. A., Gedan, K. B., Tully, K. L., Fagherazzi, S., McDowell, N. G., Molino, G. D., Pratt, D., Reay, W. G., and Stotts, S. (2025). Feedbacks regulating the salinization of coastal landscapes. *Annual Review of Marine Science*, *17*, 461-484.

Klemas, V. (2013). Remote sensing of coastal wetland biomass: An overview. *Journal of Coastal Research*, *29*, 1016-1028.

Kumar, A., Bhattacharya, T., Mukherjee, S., and Sarkar, B. (2022). A perspective on biochar for repairing damages in the soil–plant system caused by climate change-driven extreme weather events. *Biochar*, *4*, 22.

Li, Y. Q., Chai, Y. H., Wang, X. S., Huang, L. Y., Luo, X. M., Qiu, C., Liu, Q. H., and Guan, X. Y. (2021). Bacterial community in saline cropland soil on the Tibetan plateau: Responding to salinization while resisting extreme environments. *BMC Microbiology*, *21*, 1-14.

Lim, S. S., Yang, H. I., Park, H. J., Park, S. I., Seo, B. S., Lee, K. S., Lee, S. H., Lee, S. M., Kim, H. Y., Ryu, J. H., Kwak, J. H., and Choi, W. J. (2020). Land-use management for sustainable rice production and carbon sequestration in reclaimed coastal tideland soils of South Korea: A review. *Soil Science and Plant Nutrition*, *66*, 60-75.

doi:10.6342/NTU202502856

Maas, E. V., Hoffman, G. J., Chaba, G. D., Poss, J. A., and Shannon, M. C. (1983). Salt sensitivity of corn at various growth stages. *Irrigation Science*, *4*, 45-57.

Machado, R. M. A., and Serralheiro, R. P. (2017). Soil salinity: effect on vegetable crop growth. Management practices to prevent and mitigate soil salinization. *Horticulturae*, *3*, 30.

Marton, J. M., Herbert, E. R., and Craft, C. B. (2012). Effects of salinity on denitrification and greenhouse gas production from laboratory-incubated tidal forest soils. *Wetlands*, *32*, 347-357.

Mazhar, S., Pellegrini, E., Contin, M., Bravo, C., and De Nobili, M. (2022). Impacts of salinization caused by sea level rise on the biological processes of coastal soils-A review. *Frontiers in Environmental Science*, 1212.

McCauley, A., Jones, C., and Jacobsen, J. (2009). Soil pH and organic matter. *Nutrient Management Module*, *8*, 1-12.

Mirlas, V., Anker, Y., Aizenkod, A., and Goldshleger, N. (2022). Irrigation quality and management determine salinization in Israeli olive orchards. *Geoscientific Model Development*, *15*, 129-143.

Mukhopadhyay, R., Sarkar, B., Jat, H. S., Sharma, P. C., and Bolan, N. S. (2021). Soil salinity under climate change: Challenges for sustainable agriculture and food security. *Journal of Environmental Management*, *280*, 111736.

doi:10.6342/NTU202502856

Nordio, G., and Fagherazzi, S. (2024). Evapotranspiration and rainfall effects on post-storm salinization of coastal forests: Soil characteristics as important factor for salt-intolerant tree survival. *Water Resources Research*, *60*, e2024WR037907.

Ohenhen, L. O., Shirzaei, M., Ojha, C., and Kirwan, M. L. (2023). Hidden vulnerability of US Atlantic coast to sea-level rise due to vertical land motion. *Nature Communications*, *14*, 2038.

Okur, B., and Örçen, N. (2020). Chapter 12 Soil salinization and climate change. In M. N. V. Prasad and M. Pietrzykowski (Eds.), *Climate change and soil interactions* (pp. 331–350). Elsevier. Amsterdam, Netherlands.

Paul, K. I., Cunningham, S. C., England, J. R., Roxburgh, S. H., Preece, N. D., Lewis, T., Brooksbank, K., Crawford, D. F., and Polglase, P. J. (2016). Managing reforestation to sequester carbon, increase biodiversity potential and minimize loss of agricultural land. *Land Use Policy*, *51*, 135-149.

Peel, M. C., McMahon, T. A., and Finlayson, B. L. (2010). Vegetation impact on mean annual evapotranspiration at a global catchment scale. *Water Resources Research*, *46*, W09508.

Redelstein, R., Dinter, T., Hertel, D., and Leuschner, C. (2018). Effects of inundation, nutrient availability and plant species diversity on fine root mass and morphology across a saltmarsh flooding gradient. *Frontiers in Plant Science*, *9*, 98.

doi:10.6342/NTU202502856

Renaud, F. G., Le, T. T. H., Lindener, C., Guong, V. T., and Sebesvari, Z. (2015). Resilience and shifts in agro-ecosystems facing increasing sea-level rise and salinity intrusion in Ben Tre Province, Mekong Delta. *Climatic Change*, *133*, 69-84.

Rengasamy, P. (2010). Soil processes affecting crop production in salt-affected soils. *Functional Plant Biology*, *37*, 613-620.

Ribeiro-Barros, A. I., Pawlowski, K., and Ramalho, J. C. (2022). Mechanisms of salt stress tolerance in Casuarina: A review of recent research. *Journal of Forest Research*, *27*, 113-116.

Riley, J. P., and Tongudai, M. (1967). The major cation/chlorinity ratios in sea water. *Chemical Geology*, *2*, 263-269.

Ruehlmann, J., and Körschens, M. (2009). Calculating the effect of soil organic matter concentration on soil bulk density. *Soil Science Society of America Journal*, *73*, 876-885.

Schweizer, S. A., Mueller, C. W., Höschen, C., Ivanov, P., and Kögel-Knabner, I. (2021). The role of clay content and mineral surface area for soil organic carbon storage in an arable toposequence. *Biogeochemistry*, *156*, 401-420.

Setia, R., Gottschalk, P., Smith, P., Marschner, P., Baldock, J., Setia, D., and Smith, J. (2013). Soil salinity decreases global soil organic carbon stocks. *Science of The*

doi:10.6342/NTU202502856

Total Environment, *465*, 267-272.

Singh, K. (2016). Microbial and enzyme activities of saline and sodic soils. *Land Degradation & Development*, *27*, 706-718.

Shahid, S. A., Zaman, M., and Heng, L. (2018). Chapter3 Salinity and sodicity adaptation and mitigation options. In M. Zaman, S. A. Shahid, and L. Heng (Eds.), *Guideline for salinity assessment, mitigation and adaptation using nuclear and related techniques* (pp. 55-89). Springer Nature. Cham, Switzerland.

Shete, M., Rutten, M., Schoneveld, G.C., and Zewude, E. (2016). Land-use changes by large-scale plantations and their effects on soil organic carbon, micronutrients and bulk density: empirical evidence from Ethiopia. *Agriculture and Human Values*, *33*, 689-704.

Smart, L. S., Taillie, P. J., Poulter, B., Vukomanovic, J., Singh, K. K., Swenson, J. J., Mitasova, H., Smith, J. W., and Meentemeyer, R. K. (2020). Aboveground carbon loss associated with the spread of ghost forests as sea levels rise. *Environmental Research Letters*, *15*, 104028.

Sonmez, S., Buyuktas, D., Okturen, F., Citak, S. (2008). Assessment of different soil to water ratios (1:1, 1:2.5, 1:5) in soil salinity studies. *Geoderma*, *144*, 361-369.

Spencer, T., Schuerch, M., Nicholls, R. J., Hinkel, J., Lincke, D., Vafeidis, A. T., Reef, R., McFadden, L., and Brown, S. (2016). Global coastal wetland change under sea-

doi:10.6342/NTU202502856

level rise and related stresses: The DIVA Wetland Change Model. *Global and Planetary Change*, *139*, 15-30.

Sun, D., and Dickinson, G. R. (1995). Survival and growth responses of a number of Australian tree species planted on a saline site in tropical north Australia. *Journal of Applied Ecology*, *32*, 817-826.

Teixeira, M. C., Vitória, A. P., de Rezende, C. E., de Almeida, M. G., and Nardoto, G. B. (2020). Consequences of removal of exotic species (eucalyptus) on carbon and nitrogen cycles in the soil-plant system in a secondary tropical Atlantic forest in Brazil with a dual-isotope approach. *PeerJ*, *8*, e9222.

Tomar, O. S., and Gupta, R. K. (2002). Relative performance of some accessions of Casuarina spp. and silvicultural practices on saline waterlogged soils in semiarid conditions. *Arid Land Research and Management*, *16*, 177-184.

Ullman, J. L. (2013). *Soil salinity in agricultural systems: The basics. Strategies for minimizing salinity problems and optimizing crop production in-service training, Hastings, FL.* Agricultural and Biological Engineering, University of Florida, Gainesville, USA. Accessed July 11, 2025. From: https://hos.ifas.ufl.edu/media/hosifasufledu/documents/pdf/in-service-training/ist30688/IST30688---7.pdf

van de Wal, R., Melet, A., Bellafiore, D., Camus, P., Ferrarin, C., Oude Essink, G.,

doi:10.6342/NTU202502856

Haigh, I. D., Lionello, P., Luijendijk, A., Toimil, A., Staneva, J., and Vousdoukas, M. (2024). *Sea level rise in Europe: Impacts and consequences* (Chapter 5). In B. van den Hurk, N. Pinardi, T. Kiefer, K. Larkin, P. Manderscheid, and K. Richter (Eds.), *Sea level rise in Europe: 1st assessment report of the Knowledge Hub on Sea Level Rise (3-SLRE1)*. Copernicus Publications. Göttingen, Germany.

Verstraeten, W. W., Muys, B., Feyen, J., Veroustraete, F., Minnaert, M., Meiresonne, L., and De Schrijver, A. (2005). Comparative analysis of the actual evapotranspiration of Flemish forest and cropland, using the soil water balance model WAVE. *Hydrology and Earth System Sciences*, *9*, 225-241.

Wang, Y., and Li, B. (2022). Dynamics arising from the impact of large-scale afforestation on ecosystem services. *Land Degradation & Development*, *33*, 3186-3198.

Wang, Z., Zhao, G., Gao, M., and Chang, C. (2017). Spatial variability of soil salinity in coastal saline soil at different scales in the Yellow River Delta, China. *Environmental Monitoring and Assessment*, *189*, 1-12.

Wang, X., Liu, Z., Xiong, K., Li, Y., and Cheng, K. (2022). Soil organic carbon distribution and its response to soil erosion based on EEM-PARAFAC and stable carbon isotope, a field study in the rocky desertification control of South China Karst. *International Journal of Environmental Research and Public Health*, *19*,

doi:10.6342/NTU202502856

3210.

Wendelberger, K. S., and Richards, J. H. (2017). Halophytes can salinize soil when competing with glycophytes, intensifying effects of sea level rise in coastal communities. *Oecologia*, *184*, 729-737.

White, E., and Kaplan, D. (2017). Restore or retreat? Saltwater intrusion and water management in coastal wetlands. *Ecosystem Health and Sustainability*, *3*, e01258.

Wong, V. N., Greene, R. S. B., Dalal, R. C., and Murphy, B. W. (2010). Soil carbon dynamics in saline and sodic soils: a review. *Soil Use and Management*, *26*, 2-11.

Xiao, C., Gong, Y., Pei, X., Chen, H., Li, S., Lu, C., Chen, L., Zheng, X., Zheng, J., and Yan, X. (2024). Impacts of Land-Use Change from Primary Forest to Cropland on the Storage of Soil Organic Carbon. *Applied Sciences*, *14*, 4736.

Xing, G., Wang, X., Jiang, Y., Yang, H., Mai, S., Xu, W., Hou, E., Huang, X., Yang, Q., Liu, W., and Long, W. (2023). Variations and influencing factors of soil organic carbon during the tropical forest succession from plantation to secondary and old–growth forest. *Frontiers in Ecology and Evolution*, *10*, 1104369.

Xu, Z., Zuo, L., Zhang, Y., Huang, R., and Li, L. (2022). Is allelochemical synthesis in Casuarina equisetifolia plantation related to litter microorganisms?. *Frontiers in Plant Science*, *13*, 1022984.

Yang, C., Li, J., and Zhang, Y. (2019). Soil aggregates indirectly influence litter carbon

doi:10.6342/NTU202502856

storage and release through soil pH in the highly alkaline soils of north China. *PeerJ*, *7*, e7949.

Yao, Y., Chen, J., Li, F., Sun, M., Yang, X., Wang, G., Ma, J., and Sun, W. (2022). Exchangeable Ca^{2+} content and soil aggregate stability control the soil organic carbon content in degraded Horqin grassland. *Ecological Indicators*, *134*, 108507.

Yin, C. Y., Zhao, J., Chen, X. B., Li, L. J., Liu, H., and Hu, Q. L. (2022). Desalination characteristics and efficiency of high saline soil leached by brackish water and Yellow River water. *Agricultural Water Management*, *263*, 107461.

Zahran, H. H. (1997). Diversity, adaptation and activity of the bacterial flora in saline environments. *Biology and Fertility of Soils*, *25*, 211-223.

Zhang, Y., Hou, K., Qian, H., Gao, Y., Fang, Y., Xiao, S., Tang, S., Zhang, Q., Qu, W., and Ren, W. (2022). Characterization of soil salinization and its driving factors in a typical irrigation area of Northwest China. *Science of the Total Environment*, *837*, 155808.

doi:10.6342/NTU202502856

Appendix

$$\text{ESR} = \frac{Exchangeable\ Na^{+}}{Exchangeable\ Ca^{2+} + Exchangeable\ Mg^{2+}}$$

(formula A1, unit of concentration: cmol kg^{-1})

Table A1. Soil Exchangeable Sodium Ratio of Aogu Wetland

Soil Properties	Land Type	Depth (cm)	AG West	AG East	BG	GC	HSR
ESR	Forest	0-20	5.9 ± 1.8	1.8 ± 0.8	0.9 ± 0.3	0.4 ± 0.2	0.01 ± 0.2
		20-40	2.3 ± 0.1	1.9 ± 0.5	1.1 ± 0.3	0.4 ± 0.1	0.01 ± 0.0
		40-60	3.3 ± 0.2	2.5 ± 0.5	0.7 ± 0.1	0.4 ± 0.05	-
		60-80	2.7 ± 0.3	5.0 ± 0.8	1.1 ± 0.3	0.5 ± 0.1	-
		80-100	2.1 ± 0.1	3.8 ± 0.2	1.5 ± 0.4	0.5 ± 0.1	-
	Cropland	0-20	0.9 ± 0.2	0.1 ± 0.03	0.1 ± 0.03	0.2 ± 0.1	0.01 ± 0.0
		20-40	0.9 ± 0.1	0.1 ± 0.04	0.1 ± 0.04	0.2 ± 0.1	0.02 ± 0.0
		40-60	0.7 ± 0.2	0.05 ± 0.04	0.1 ± 0.04	0.2 ± 0.02	-
		60-80	0.7 ± 0.3	0.1 ± 0.03	0.1 ± 0.03	0.3 ± 0.1	-
		80-100	0.8 ± 0.5	0.1 ± 0.01	0.1 ± 0.02	0.2 ± 0.03	-

doi:10.6342/NTU202502856